

## Analysis of Chiral Mean-Field Models for Nuclei

R. J. Furnstahl

*Department of Physics*

*The Ohio State University, Columbus, Ohio 43210*

Brian D. Serot

*Department of Physics and Nuclear Theory Center*

*Indiana University, Bloomington, Indiana 47405*

Hua-Bin Tang\*

*Department of Physics*

*The Ohio State University, Columbus, Ohio 43210*

(November, 1995)

### Abstract

An analysis of nuclear properties based on a relativistic energy functional containing Dirac nucleons and classical scalar and vector meson fields is discussed. Density functional theory implies that this energy functional can include many-body effects that go beyond the simple Hartree approximation. Using basic ideas from effective field theory, a systematic truncation scheme is developed for the energy functional, which is based on an expansion in powers of the meson fields and their gradients. The utility of this approach relies on the observation that the large scalar and vector fields in nuclei are small enough compared to the nucleon mass to provide useful expansion parameters, yet large enough that exchange and correlation corrections to the fields can be treated as minor perturbations. Field equations for nuclei and nuclear matter are obtained by extremizing the energy functional with respect to the field variables, and inversion of these field equations allows one to express the unknown coefficients in the energy functional directly in terms of nuclear matter properties near equilibrium. This allows for a systematic

---

\*Present address: School of Physics and Astronomy, University of Minnesota, Minneapolis, MN 55455.

and complete study of the parameter space, so that parameter sets that accurately reproduce nuclear observables can be found, and models that fail to reproduce nuclear properties can be excluded.

Chiral models are analyzed by considering specific lagrangians that realize the spontaneously broken chiral symmetry of QCD in different ways and by studying them at the Hartree level. The resulting energy functionals are special cases of the general functional considered earlier. Models that include a light scalar meson playing a dual role as the chiral partner of the pion and the mediator of the intermediate-range nucleon–nucleon interaction, and which include a “Mexican-hat” potential, fail to reproduce basic ground-state properties of nuclei at the Hartree level. In contrast, chiral models with a *nonlinear* realization of the symmetry are shown to contain the full flexibility inherent in the general energy functional and can therefore successfully describe nuclei.

## I. INTRODUCTION

There is a long history of attempts to unite relativistic mean-field phenomenology with manifest chiral symmetry. In particular, it has been tempting to build upon the linear sigma model [1–3], where a light scalar meson plays a dual role as the chiral partner of the pion *and* the mediator of the intermediate-range nucleon–nucleon (NN) attraction [4–16]. In earlier work [17], we surveyed a broad class of these chiral hadronic models and observed that they fail to reproduce basic properties of finite nuclei at the Hartree level. In this paper, we demonstrate the generic failure of this type of model using a more complete approach [18] for analyzing the relationship between model parameters and nuclear observables. We also illustrate the characteristics of chiral models that *can* successfully describe finite nuclei.

We base our analysis on an energy functional, which depends on valence-nucleon Dirac wave functions and classical scalar and vector meson fields. Extremizing the functional leads to coupled equations for finite nuclei and nuclear matter [see Eqs. (1)–(6)]. The successes of relativistic mean-field models have shown that these variables (nucleon, scalar, vector) allow an efficient and natural description of bulk and single-particle nuclear properties [19–27].

Although the energy functional contains classical meson fields, this framework can accommodate physics beyond the simple Hartree (or one-baryon-loop) approximation. This is achieved by combining aspects of both density functional theory (DFT) [28–31] and effective field theory (EFT) [32–34]. In a DFT formulation of the relativistic nuclear many-body problem, the central object is an energy functional of scalar and vector densities (or more generally, vector four-currents). Extremization of the functional gives rise to Dirac equations for occupied orbitals with *local* scalar and vector potentials, not only in the Hartree approximation, but in the general case as well.<sup>1</sup> Rather than work solely with the densities, we can introduce auxiliary variables corresponding to the local potentials, so that the functional depends also on meson fields. The resulting DFT formulation takes the form of a Hartree calculation, but correlation effects can be included, *if* the proper density functional can be found. Our procedure is analogous to the well-known Kohn–Sham [35] approach in DFT, with the local meson fields playing the role of Kohn–Sham potentials; by introducing nonlinear couplings between these fields, we can implicitly include density dependence in the single-particle potentials.

Moreover, by introducing the meson fields, we can incorporate the ideas of EFT. The exact energy functional has kinetic energy and Hartree parts (which are combined in the relativistic formulation) plus an “exchange-correlation” functional, which is a nonlocal, non-analytic functional of the densities that contains all the other many-body and relativistic effects. We do not try to construct the latter functional explicitly from a lagrangian (which would be equivalent to solving the full many-body problem), nor do we attempt here to construct an explicit functional using standard many-body techniques [30]. Rather, we approximate the functional using an expansion in classical meson fields and their derivatives. The parameters introduced in the expansion can be fit to experiment, and if we have a

---

<sup>1</sup>Note that the Dirac eigenvalues do not correspond precisely to physical energy levels in the general case [28].

systematic way to truncate the expansion, the framework is predictive. Thus a conventional mean-field energy functional fit directly to nuclear properties, if allowed to be sufficiently general, will automatically incorporate effects beyond the Hartree approximation, such as those due to short-range correlations.

We rely on the special characteristics of nuclear ground states in a relativistic formulation, namely, that the mean scalar and vector potentials  $\Phi$  and  $W$  are large on nuclear energy scales but are small compared to the nucleon mass  $M$  and vary slowly in finite nuclei [18,36]. This implies that the ratios  $\Phi/M$  and  $W/M$  and the gradients  $|\nabla\Phi|/M^2$  and  $|\nabla W|/M^2$  are useful expansion parameters. Moreover, as is illustrated in Dirac–Brueckner–Hartree–Fock (DBHF) calculations [37–39], the scalar and vector potentials (or self-energies) are nearly state independent and are dominated by the Hartree contributions. Thus the Hartree contributions to the energy functional should dominate, and an expansion of the exchange–correlation functional in terms of mean fields should be a reasonable approximation. This “Hartree dominance” also implies that it should be a good approximation to associate the single-particle Dirac eigenvalues with the observed nuclear energy levels, at least for states near the Fermi surface [28]. Of course, the mean-field expansion cannot accommodate all of the nonlocal and nonanalytic aspects of the exchange–correlation functional; however, we reserve a complete discussion of the limits of this approach for future work [40].

The mean-field energy functional is specified by the values of various coupling constants and masses. These parameters can be constrained in two ways. First, the energy functional provides a framework for relating model parameters to appropriate nuclear observables. This translates empirical nuclear properties into conditions on acceptable parametrizations. In practice, nuclei provide rather stringent constraints. On the other hand, the realization of QCD symmetries (such as chiral symmetry) in a candidate model lagrangian may impose relationships between parameters in the corresponding Hartree approximation to the energy functional. Our goal in this work is to test whether the two sets of constraints are compatible.

We begin by analyzing a general energy functional to determine the characteristics that generate successful phenomenology. An essential element is a plausible truncation scheme, so that the functional does not entail an unrestricted number of parameters. As indicated earlier, our basic expansion parameters are  $\Phi/M$  and  $W/M$ , where  $\Phi$  and  $W$  correspond to the potentials in the single-particle Dirac equations [see Eq. (6)]. We define success through a set of nuclear observables that should be quantitatively reproduced in any useful description of ground-state properties. These observables include: 1) nuclear shape properties, such as charge radii and charge densities, 2) nuclear binding-energy systematics, and 3) single-particle properties such as level spacings and orderings, which reflect spin-orbit splittings and shell structure. If one recalls that the Kohn–Sham approach is formulated to reproduce precisely the ground-state density, and that the Hartree contributions are expected to dominate the Dirac single-particle potentials, *these observables are precisely the ones for which meaningful comparisons with experiment should be possible*. Moreover, experience has shown that these observables can be replaced by a set of nuclear matter properties plus constraints on the meson masses [19–21,23,24]. While the parameters of a general functional are not completely determined by requiring these properties to be reproduced, regions in parameter space that generate realistic nuclei can clearly be identified.

The second part of our analysis is to examine specific chiral models that adopt a particular realization of chiral symmetry at the lagrangian level *and* a particular mechanism

for spontaneous symmetry breaking. These two features restrict the accessible regions of parameter space, and we can simply compare with the regions determined in the first part of our analysis to see if there is an overlap. We stress that in this part of the analysis, we actually start with an explicit lagrangian and construct the energy functional by working strictly in the Hartree approximation; thus, the effects of correlations in these chiral models, for example, are beyond our analysis. Nevertheless, the Hartree energy functionals are simply special cases of the general functional considered above, so we can apply our earlier results.

The most important ingredient is a procedure that can systematically connect the nuclear observables and the model parameters. In previous analyses, the mean-field parameters have been determined either by fitting nuclear matter equilibrium properties plus some input from finite nuclei (*e.g.*, the rms radius of  $^{40}\text{Ca}$ ) or by optimizing the predictions of selected experimental observables across the Periodic Table (using a  $\chi^2$  measure, for example). These procedures are useful if the goal is to find a good description of nuclei for a given model, but not if we want to rule out a class of models. In particular, it is difficult to search through the parameter space to determine where the boundaries of acceptable parametrizations lie. This severely limits qualitative insight and solid conclusions.

The first approach was followed in our previous studies of linear sigma models: we explored the chiral-model parameter space by fitting to nuclear matter equilibrium properties and then by calculating finite nuclei for what we hoped was an exhaustive range of parameter sets. In the present work, we invert this analysis by adapting the approach developed by Bodmer [18], which enables us to use basic nuclear properties, derived from the observables, *to solve directly for the model parameters*. Since there are only a few basic properties that provide meaningful constraints, the resulting conditions are undercomplete for the most general functionals, and there are families of acceptable solutions defined by regions in the parameter space. Specific models, however, introduce relations among some parameters and set others to zero, so that in the accessible region of parameter space there may be no acceptable descriptions of nuclei. Thus one way a model can fail is if there is no overlap between the accessible and desirable regions of parameter space.

There is another way a model can fail, which arises from the nonlinear meson interactions in the energy functional and in the resulting meson field equations. For some models and some parameter sets, one can find a nuclear ground state that has the appropriate properties at equilibrium, but this ground state exists only over a narrow range of nuclear densities. If the ground state fails to exist at densities that have clearly been obtained experimentally (say, slightly higher than normal nuclear matter density), the disappearance of the model ground state must also be considered a failure of the model. We will make these considerations more precise as we proceed.

The results of the present analysis solidify our previous conclusion [17] that chiral hadronic models built upon the conventional linear sigma model cannot reproduce observed properties of finite nuclei in the Hartree approximation. The main problems in these linear sigma models arise from the nonlinear terms in the “Mexican-hat” potential, which serves to precipitate spontaneous symmetry breaking, and from the large pion coupling. The consequences are a scalar meson mass that is too large and density-dependent forces (in the form of scalar self-couplings) with the wrong systematics. These problems are not remedied by including one-baryon-loop vacuum corrections or by adding parameters that generalize

the model.

On the other hand, chiral models that *are* phenomenologically successful can be constructed. As an example, we discuss a model that was introduced in a recent paper [36], which features a nonlinear realization of chiral symmetry.

For a model to be viable, it should also exhibit “naturalness” in the fitted parameters. Here, naturalness implies that the coefficients of the various terms in the energy functional, when expressed in appropriate dimensionless form, should all be of order unity. This means that we can anticipate the approximate magnitude of contributions to the energy functional (at least up to moderate nuclear densities) and thereby motivate a suitable expansion and truncation scheme for the functional; if the coefficients are natural, the omitted terms will be numerically unimportant. The naturalness of our effective field theory also implies that one should include all possible terms (that is, those allowed by the symmetries) through a given order of truncation; it is *unnatural* for some coefficients to vanish without an appropriate symmetry argument. One consequence is that nonlinear interactions of the vector field should play an important role in providing a good and natural fit to nuclei, and we indeed find that this is the case. We stress this point because nearly all investigations of relativistic mean-field phenomenology to date [41,21–24,26,27] have arbitrarily restricted consideration to scalar self-interactions only.<sup>2</sup> The quartic vector self-coupling has been included in phenomenological calculations only recently [18,42,43].

There are many studies in the literature that have characterized the nature of phenomenologically successful mean-field models, including Refs. [21–24,26,27]. We echo many of the common conclusions, such as the necessity for a small nucleon effective mass ( $0.58 \lesssim M^*/M \lesssim 0.64$ ) at equilibrium density and for a scalar meson mass of roughly 500 MeV. Nevertheless, since previous analyses typically determined the model parameters through a fitting procedure that simply calculates nuclei repeatedly until a “good fit” is obtained, connections between nuclear observables and the resulting parameters are somewhat obscure. Through our analysis, we try to demystify the connections between the observables and the parameters, so that the structure of the resulting energy functionals can be better understood.

The original motivation for this work was to expand upon our previous analyses of linear chiral models [17] and thereby solidify our earlier conclusions. In carrying out this program, however, we were forced to extend our mean-field machinery in several different directions. It is important to emphasize these new aspects, which are more general than the chiral-model analysis, and which in fact comprise the most important results in this paper. First, by starting from an energy functional containing baryons and classical scalar and vector fields, we have a framework that goes beyond the simple Hartree approximation. This follows because we can interpret the analysis in the context of density functional theory and an associated (relativistic) Kohn–Sham approach. Second, although it is possible to vary the parameters

---

<sup>2</sup>Some previous analyses were based on *renormalizable* scalar–vector theories, for which such restrictions are appropriate. If renormalizability is abandoned, however, as in an effective field theory, there is no reason to omit vector–vector and scalar–vector interactions. (See the comments below on vector self-interactions, spin content, and causality.)

in the energy functional until desirable properties of nuclear matter and finite nuclei are obtained, it is more efficient to invert the field equations and express the model parameters directly in terms of the desired observables. This allows for a systematic investigation of the parameter space and clarifies the relationships between observables and model parameters. Finally, by applying ideas from effective field theory, such as the importance of naturalness and a suitable expansion scheme, to the construction of the ground-state energy functional, we find that it is important and necessary to include all allowable terms in the functional at the chosen level of truncation. This modern view of relativistic quantum field theory [34] generalizes earlier approaches based on renormalizable theories [44,45,20,25] and allows for a more unified discussion of relativistic approaches to the nuclear many-body problem.

The paper is organized as follows: In Section II, we consider a general energy functional (not manifestly chiral) and characterize phenomenologically successful models. In Section III, we show how empirical properties of nuclear matter and finite nuclei can be used directly to determine or to constrain the parametrizations of candidate energy functionals. We also illustrate how to map out the parameter space. In Section IV, we specialize the analysis to models built on the linear sigma model with a “Mexican-hat” potential and demonstrate their generic failure at the Hartree level. In Section V, we consider a chiral model that successfully describes finite nuclei. Section VI has some additional discussion, including the general strategy that justifies the expansion and truncation scheme. Section VII is a summary.

## II. ENERGY FUNCTIONALS AND NUCLEAR PROPERTIES

Our first goal is to construct an energy functional whose extremization accurately reproduces bulk and single-particle nuclear observables. Experience with relativistic mean-field models shows that scalar and vector mesons with appropriate masses lead to NN interactions with the desired ranges, and that by introducing nonlinearities in the meson fields, we can include density dependence in these interactions [41,19,18]. We assume that the nuclear ground states have good parity and are invariant under time reversal, which implies that a classical pion field does not appear<sup>3</sup> [22]. Furthermore, we retain only the valence nucleons explicitly. This does not mean that we are *neglecting* pionic or vacuum effects, but rather that they are implicitly contained in the coefficients of the energy functional. This is discussed for one-loop vacuum contributions in Ref. [36] and in Sec. V; a more general discussion will be given elsewhere [40].

As emphasized in the Introduction, while our energy functional can be interpreted as arising from a hadronic lagrangian treated in the Hartree approximation, it can also be interpreted as an approximation to a general density functional that incorporates all correlation effects. This approach is particularly compelling because of the dominance of Hartree effects in the relativistic approach. This claim is supported by Dirac–Brueckner–Hartree–Fock (DBHF) calculations, which indicate that exchange terms and short-range correlations

---

<sup>3</sup>When odd- $A$  nuclei are studied using mean-field models, time-reversal invariance is broken explicitly, which leads to pion mean fields.

do not significantly change the size of the Hartree self-energies nor introduce strong state dependence (at least for occupied states) [46,37]. By determining the model parameters from finite-density bulk and single-particle observables instead of from NN scattering, and by explicitly allowing meson nonlinearities that generate additional density dependence, we automatically include the most important effects of correlations. In fact, one can choose the nonlinear meson parameters so that the mean fields reproduce the scalar and vector self-energies obtained in a DBHF calculation [42].

We start with a mean-field energy functional for spherically or axially symmetric ground states that generalizes the functional used in Ref. [22]. It depends on a set of single-particle Dirac wave functions  $U_\nu(\mathbf{x})$  (labeled by quantum numbers  $\nu$ ) for the occupied valence orbitals and on classical, static meson fields  $\phi(\mathbf{x})$  and  $V_0(\mathbf{x})$ . It can be written as

$$\begin{aligned}
E[\{U_\nu\}, \phi, V_0] = & \int d^3x \left( \sum_\nu^{\text{occ}} U_\nu^\dagger(\mathbf{x}) \{ -i\boldsymbol{\alpha} \cdot \nabla + \beta[M - g_s\phi(\mathbf{x})] + g_v V_0(\mathbf{x}) \} U_\nu(\mathbf{x}) \right. \\
& + \frac{1}{2} \{ [\nabla\phi(\mathbf{x})]^2 + m_s^2[\phi(\mathbf{x})]^2 \} - \frac{1}{2} \{ [\nabla V_0(\mathbf{x})]^2 + m_v^2[V_0(\mathbf{x})]^2 \} \\
& + \frac{1}{3!} \kappa[\phi(\mathbf{x})]^3 + \frac{1}{4!} \lambda[\phi(\mathbf{x})]^4 - \frac{1}{4!} \zeta [g_v V_0(\mathbf{x})]^4 \\
& \left. + \alpha \frac{M}{g_s} [g_v V_0(\mathbf{x})]^2 \phi(\mathbf{x}) - \frac{1}{2} \alpha' [g_v V_0(\mathbf{x})]^2 [\phi(\mathbf{x})]^2 \right), \quad (1)
\end{aligned}$$

subject to the constraint

$$\int d^3x U_\nu^\dagger(\mathbf{x}) U_\nu(\mathbf{x}) = 1, \quad (2)$$

for all occupied states. Observe that the functional has been truncated at quartic terms in the fields and at quadratic terms in gradients of the fields; this truncation will be justified below.

To realistically describe finite nuclei, the functional must be extended to include rho mesons, pions, and photons. In the present discussion, however, we focus on nuclear ground-state properties that primarily constrain isoscalar physics. Thus the Coulomb contribution and a correct reproduction of the bulk symmetry energy ( $\approx 35$  MeV) are sufficient for our purposes, and this requires only the conventional extensions to include neutral rho mesons (denoted by  $b_0$ ) and the Coulomb field (see also Ref. [20]):

$$\begin{aligned}
E[\{U_\nu\}, \phi, V_0, b_0, A_0] = & E[\{U_\nu\}, \phi, V_0] + \\
& \int d^3x \left( \sum_\nu^{\text{occ}} U_\nu^\dagger(\mathbf{x}) \left\{ \frac{1}{2} g_\rho \tau_3 b_0(\mathbf{x}) + e \frac{1}{2} (1 + \tau_3) A_0(\mathbf{x}) \right\} U_\nu(\mathbf{x}) \right. \\
& \left. - \frac{1}{2} \{ [\nabla b_0(\mathbf{x})]^2 + m_\rho^2 [b_0(\mathbf{x})]^2 \} - \frac{1}{2} [\nabla A_0(\mathbf{x})]^2 \right). \quad (3)
\end{aligned}$$

For simplicity, we suppress these isovector terms in the sequel, although they are included in the numerical calculations of finite nuclei. As noted above, the chiral models of Secs. IV and V have no explicit pion field contribution in this formulation.

The meson fields are determined by requiring the functional to be stationary with respect to their variations; this yields (after partial integrations) the meson field equations



$$\begin{aligned}
(\nabla^2 - m_s^2)\phi(\mathbf{x}) &= -g_s \sum_{\nu}^{\text{occ}} \bar{U}_{\nu}(\mathbf{x}) U_{\nu}(\mathbf{x}) \\
&\quad + \frac{1}{2}\kappa[\phi(\mathbf{x})]^2 + \frac{1}{6}\lambda[\phi(\mathbf{x})]^3 + \left(\alpha\frac{M}{g_s} - \alpha'\phi(\mathbf{x})\right)[g_v V_0(\mathbf{x})]^2, \quad (4)
\end{aligned}$$

$$\begin{aligned}
(\nabla^2 - m_v^2)V_0(\mathbf{x}) &= -g_v \sum_{\nu}^{\text{occ}} U_{\nu}^{\dagger}(\mathbf{x}) U_{\nu}(\mathbf{x}) \\
&\quad + \frac{1}{6}\zeta g_v^4 [V_0(\mathbf{x})]^3 - 2\alpha\frac{M}{g_s} g_v^2 V_0(\mathbf{x})\phi(\mathbf{x}) + \alpha' g_v^2 V_0(\mathbf{x})[\phi(\mathbf{x})]^2. \quad (5)
\end{aligned}$$

The single-particle orbitals are determined similarly. The constraint equation (2) is imposed for each orbital  $U_{\nu}$  by using a Lagrange multiplier  $\epsilon_{\nu}$ , which we identify as the energy eigenvalue of the Dirac equation:

$$\{-i\boldsymbol{\alpha}\cdot\nabla + \beta[M - g_s\phi(\mathbf{x})] + g_v V_0(\mathbf{x})\}U_{\nu}(\mathbf{x}) = \epsilon_{\nu}U_{\nu}(\mathbf{x}). \quad (6)$$

The energy is minimized by solving these equations self-consistently for the  $N$  and  $Z$  lowest eigenvalues to determine the occupied neutron and proton states.

This energy functional, which provides an approximation to a general density functional, could also be derived as the one-baryon-loop energy from the lagrangian density

$$\begin{aligned}
\mathcal{L} &= \bar{\psi}[i\gamma_{\mu}\partial^{\mu} - g_v\gamma_{\mu}V^{\mu} - (M - g_s\phi)]\psi + \frac{1}{2}(\partial_{\mu}\phi\partial^{\mu}\phi - m_s^2\phi^2) \\
&\quad - \frac{1}{4}(\partial_{\mu}V_{\nu} - \partial_{\nu}V_{\mu})^2 + \frac{1}{2}m_v^2V_{\mu}V^{\mu} - \frac{1}{3!}\kappa\phi^3 - \frac{1}{4!}\lambda\phi^4 \\
&\quad + \frac{1}{4!}\zeta g_v^4 (V_{\mu}V^{\mu})^2 - \alpha g_v^2 \frac{M}{g_s} V_{\mu}V^{\mu}\phi + \frac{1}{2}\alpha' g_v^2 V_{\mu}V^{\mu}\phi^2, \quad (7)
\end{aligned}$$

by following the discussion in Ref. [36].<sup>4</sup> Alternatively, one could construct the Hartree Hamiltonian from Eq. (7) and take its expectation value in a state specified by static meson fields and a set of occupied single-nucleon orbitals (labeled by quantum numbers  $\nu$ ). In this lagrangian formulation, it appears that vacuum contributions are neglected, because the sum in  $E$  runs over valence nucleons only. However, the vacuum effects can be precisely absorbed into the coefficients of the interaction terms, provided we keep nonlinearities to all orders [36]. If we assume that a truncation at some low order of the fields and their derivatives is sufficiently accurate at nuclear densities (which we justify on the basis of naturalness), then the vacuum effects are already included with sufficient accuracy in the functional of Eq. (1).

The notation and structure of the lagrangian (7) has been chosen to conform to previous usage in the literature. It includes as special cases most of the lagrangians used in mean-field studies. The Walecka model retains the terms with nucleon fields and just the kinetic

---

<sup>4</sup>Note that this derivation of the functional starts from a *Lorentz-invariant* action  $S = \int d^4x \mathcal{L}$ . If we consider the energy functional as an effective functional, however, we presently know of no reason to exclude terms that explicitly contain the medium four-velocity  $u^{\mu}$ , such as  $u^{\mu}V_{\mu}V^{\nu}V_{\nu}$ . This issue will be considered in a later publication.

TABLE I. Relationship between parameters of Eq. (1) or Eq. (7) and specific models. Chiral models with a linear representation should have  $g_s = g_\pi$  at the level considered here; however, we will allow  $g_s = g_\pi/g_A$  with  $g_\pi \approx 13.5$  and  $g_A \approx 1.26$ , so that the Goldberger–Treiman relation is satisfied. We have also taken  $m_\pi = 0$  in writing the entries. Note that the  $\eta$ 's in the last two rows are unrelated.

Model	Ref.	$g_v$	$\kappa$	$\lambda$	$\zeta$	$\alpha$	$\alpha'$
Walecka	[44]	$g_v$	0	0	0	0	0
Nonlinear scalar	[41]	$g_v$	$-2b$	$6c$	0	0	0
Bodmer	[18]	$g_v$	$2a$	$6b$	$\frac{6m_v^2}{Z^2 g_v^2}$	0	0
Chiral $\sigma\omega$	[20]	$g_v$	$-\frac{3g_s m_s^2}{M}$	$\frac{3g_s^2 m_s^2}{M^2}$	0	0	0
Boguta	[9]	$\frac{g_s m_v}{M}$	$-\frac{3g_s m_s^2}{M}$	$\frac{3g_s^2 m_s^2}{M^2}$	0	1	1
General chiral	[17]	$g_v$	$-\frac{3g_s m_s^2}{M}$	$\frac{3g_s^2 m_s^2}{M^2}$	$\zeta$	$\eta^2$	$\eta^2$
Nonlinear chiral	[36]	$g_v$	$\frac{(3d-8)m_s^2}{dS_0}$	$\frac{(11d^2-48d+48)m_s^2}{(dS_0)^2}$	$\zeta$	$\frac{-\eta g_s}{2S_0 M} \frac{m_v^2}{g_v^2}$	0

and mass terms for the scalar and vector fields. Nonlinear terms in the scalar field were introduced long ago by Schiff [47] and later studied by Boguta and Bodmer [41]. Although widely used, a long-standing worry about such models was that the quartic scalar coupling  $\lambda$  is negative in good fits to finite nuclei [21,23,24,26].

This concern is eliminated when quartic vector self-interactions are included in the lagrangian or energy functional. Such a term was first introduced by Bodmer and Price [48,18], motivated by a search for softer high-density equations of state. Gmuca employed the quartic vector term to account for density dependence in the vector self-energy, as implied by DBHF calculations [42]. Previous studies of lagrangians with neutral vector mesons have suggested that such terms can lead to field equations with causality-violating solutions [49,50] or to the mixing of spin-one and spin-zero representations [51]. However, if  $\zeta > 0$  and the other vector parameters are natural, then there are no problems with causality. The second point is not an issue in our effective-field-theory approach; we are not describing elementary vector mesons, and we certainly expect mixing effects at finite density [45].

Equation (7) also includes as special cases all of the chiral models considered in Ref. [17] and the chiral model of Ref. [36].<sup>5</sup> The relationships between parameters in Eq. (7) and models from the literature are summarized in Table I.

While our immediate intent is to work with a functional that includes the chiral models as special cases, the proposed functional (1) is actually more general than it appears at first. One can imagine several classes of additional terms in Eq. (7):

---

<sup>5</sup>The model of Ref. [36] actually contains a logarithmic potential for the scalar field, which means an infinite polynomial in  $\phi$ . However, for reasons discussed below, specifying the cubic and quartic terms determines the energy functional at ordinary densities at a level sufficient for our purposes.

1. Higher-order self-couplings and derivatives involving meson fields alone [*e.g.*,  $\phi^5$  or  $(V^\mu V_\mu)^3$  or  $(\partial_\mu \phi \partial^\mu \phi)^2$ ];
2. Contact terms involving nucleon fields beyond bilinear order [*e.g.*,  $(\bar{\psi}\psi)^2$ ];
3. More complicated meson–nucleon couplings [*e.g.*,  $g_s(\phi)\bar{\psi}\psi\phi$ ].

Let us consider each in turn.

For applications of the energy functional to ordinary nuclei, contributions to the energy from higher-order polynomials (beyond quartic) or higher-order gradient terms (beyond quadratic) are numerically small, unless the coefficients are “unnaturally” large. The definition of naturalness proposed here (and discussed further in Sec. VI) is simple: when written in appropriate dimensionless form, the coefficients of all mesonic terms in  $E$  are of order unity. Thus we can organize our truncation by counting powers of the local scalar and vector potentials (or self-energies) that appear in the single-particle Dirac equations, divided by the nucleon mass, and by counting gradients of the potentials divided by the square of the mass. We take as a basic principle that our functional *implicitly* includes higher-order terms, but with natural coefficients, which can be ignored in practice at ordinary nuclear densities and below; their small contributions can be absorbed into slight adjustments of the other coefficients. Thus we have the possibility of a useful expansion and truncation scheme in this framework. We must establish, however, after determining the parameters, that the highest-order terms retained do not dominate the energy, and that adding additional terms produces only small changes in the parameters. These considerations and the consequences of this approach for extrapolations to high density are discussed in Sec. VI.

Contact terms arise if we “integrate out” the scalar and vector fields (by using the field equations, for example). Conversely, contact terms included originally in the energy functional (excluding certain terms with derivatives) can be eliminated in favor of the scalar and vector fields, if we allow products of fields to all orders. The issue then really becomes one of efficiency, since in either framework one will have to truncate in practice. Based on the economical successes of relativistic meson-exchange phenomenology and to connect to specific models, we use the field expansion. We again rely on the naturalness of the coefficients to motivate a truncation at fourth order in the fields.<sup>6</sup> Further discussion and development of these ideas will be given in a future paper [40].

Models have been proposed that replace  $M^* = M - g_s\phi$  in the lagrangian by a more general function  $M^*(\phi)$  [or equivalently, that make the replacement  $g_s \rightarrow g_s(\phi)$ ] [52–54]. This function must have a Taylor expansion around vanishing  $\phi$ , but is otherwise quite general in principle. More generally, the Yukawa couplings of the scalar and vector to the nucleon fields can be replaced by polynomials in  $\phi$  and  $V^\mu$  (in Lorentz-invariant combinations). The motivation for such models is often that these terms are needed to reflect the compositeness of the nucleon. However, if we allow arbitrary polynomials in the meson fields in our functional, we can simply *redefine* the fields to eliminate non-Yukawa couplings to the nucleon.

---

<sup>6</sup>Strictly speaking, in this approach  $m_\nu$  should be a fit parameter rather than fixed at the physical  $\omega$  meson mass. We rely on resonance dominance and the insensitivity of the functional to the precise value of this mass to justify fixing it.

(For example, we can replace  $\phi \rightarrow \tilde{\phi}$  where  $M^*(\phi) \equiv M - g'_s \tilde{\phi}$ .) The new functional has the same form as Eq. (1), including all orders in the fields alone. The observables are unchanged by the transformation, and the only question is again one of efficiency, that is, whether a truncation to fourth order in the fields is an accurate numerical approximation.

Thus, by working with Eq. (1), we accommodate a wide class of effective models. To start our analysis, we identify the nuclear observables that we wish our functional to reproduce. The properties of finite nuclei fall into three major categories:

1. Nuclear shapes. This includes the basic manifestations of nuclear saturation [55,56]: a flat interior, a surface thickness independent of the baryon number  $B$ , and a systematic increase of the nuclear radius with  $B^{1/3}$ . These features are seen experimentally in the charge radius and the charge density; the latter is most clearly analyzed for this purpose in momentum space (*i.e.*, the form factor).
2. Binding-energy systematics. The binding energies of (closed-shell) nuclei across the periodic table must reflect the liquid-drop systematics of the basic semi-empirical mass formula. At a coarse level, this involves the sensitive interplay of the bulk binding energy ( $a_1$ ), the surface energy ( $a_2$ ), the Coulomb energy ( $a_3$ ), and the bulk symmetry energy ( $a_4$ ) (with a surface correction included) [55–58]:<sup>7</sup>

$$E/B - M = -a_1 + a_2 B^{-1/3} + a_3 \frac{Z^2}{B^{4/3}} + a_4 \frac{(N - Z)^2}{B^2(1 + 3.28/B^{1/3})}. \quad (8)$$

3. Single-particle properties. The single-particle potential is reflected in the ordering and spacing of single-particle levels, which are reasonably well identified experimentally (up to rearrangement effects that are comparatively small). Speaking in nonrelativistic language (since the Dirac equation can always be recast in “Schrödinger-equivalent” form), the level ordering in  $\ell$  implies a central potential that interpolates between a harmonic oscillator and square well. In addition, the spin-orbit potential must be strong enough to ensure the correct shell closures, but not too strong, or else the systematics of nuclear deformations will not be reproduced [22]. Finally, there is the energy dependence of the optical potential at low energies, which is related to the vector self-energy at the relativistic mean-field level [20].

One could add other properties to this list. In many cases, however, these additional properties are strongly correlated with the features listed above and so are reproduced without imposing further conditions.

Using properties of nuclei as constraints, however, is difficult in the sort of direct analysis we seek. We will therefore extrapolate from the systematics of actual observables (such as binding energies, rms radii, and spin-orbit splittings) and impose conditions on the functional *in nuclear matter* near the equilibrium density. First, nuclear matter must exhibit a

---

<sup>7</sup>There are much more sophisticated mass formulas incorporating additional physics, but this is the appropriate level of detail for our purpose.

particular equilibrium density ( $\rho_0$ ) and binding energy ( $e_0$ ) within a fairly narrow range.<sup>8</sup> These conditions are supported by calculations in relativistic models that are fit directly to properties of finite nuclei, which consistently predict similar  $\rho_0$  and  $e_0$  when extrapolated to infinite nuclear matter [23,26].

We can also consider derivatives of the energy with respect to the density evaluated at equilibrium. The second derivative or curvature determines the compression modulus ( $K_0$ ). Even though the range in  $K_0$  consistent with nuclear properties is fairly broad (approximately 200–300 MeV), this provides significant constraints on mean-field models. The most direct effect of the compressibility on ground-state properties is through the surface energy and is therefore manifested in the energy systematics. The surface energy is also correlated with the scalar mass.

The importance of higher derivatives of the energy is unclear at present. Recent work has suggested that the ratio of the “skewness” (related to the third derivative) to the compression modulus is well determined by nuclear monopole vibrations [59,60]. We do not use skewness to constrain the energy functional in this investigation, but we comment on the correlation between skewness and ground-state properties in Sec. VI. Note that one can easily extend the analysis described in Sec. III to exploit additional constraints of this type.

To correctly reproduce empirical single-particle energies, the most important ingredient beyond the depth and shape of the effective central potential is the strength of the spin-orbit interaction. In relativistic models, the spin-orbit splittings are highly correlated with the nucleon effective mass  $M^*$ . An upper bound on  $M^*$  is given by the reproduction of the shell closures in heavy nuclei and the splittings of spin-orbit pairs in light nuclei, while the reproduction of deformation systematics gives a lower bound [22]. In conjunction with the other constraints,<sup>9</sup>  $M_0^*/M$  must be in a fairly narrow interval around 0.6.

The symmetry energy is determined by the observed energy systematics [through Eq. (8)], the relative energies of proton and neutron single-particle levels in heavy nuclei [19], and isotope shifts in neutron-rich nuclei [26,61]. These imply that  $a_4 \approx 35$  MeV, with an uncertainty of several MeV.

Finally, there are important restrictions on the ranges of the attractive and repulsive interactions, or equivalently, on the momentum dependence of the scalar and vector fields. These conditions do not impact nuclear matter (since the momentum transfer is zero at the mean-field level) but are critical in finite nuclei. The major constraint is on the scalar mass, which is consistently found from direct fits to be in the vicinity of 500 MeV (when the vector mass is taken to be the physical  $\omega$  mass). Significantly larger scalar masses produce unobserved oscillations in the charge density and too steep a surface in the effective central potential, which leads to incorrect level orderings. We will assess the importance

---

<sup>8</sup>We will use the convention that properties and fields evaluated at equilibrium density are denoted with a subscript “0”.

<sup>9</sup>Spin-orbit strength is not the only source of constraints on  $M^*$ . Reinhard *et al.* concluded that  $M_0^*/M$  must be roughly 0.6 from detailed fits to finite nuclei that *did not* include the spin-orbit splittings as input [21].

of this constraint for chiral models (and the success of the nuclear matter constraints) by calculating finite nuclei after the nuclear matter analysis.

One may ask: at what level of accuracy should we require nuclear observables to be reproduced? The answer depends on the planned application of the model and the goals of the analysis. For comparison with nuclear scattering experiments, accurate nuclear densities and wave functions are required, but total binding energies are not particularly important; in contrast, for studying fission barriers or the properties of nuclei near the “drip lines”, energy systematics are paramount. Since our goal is to exclude some classes of mean-field models, we will impose less stringent constraints. The nuclear matter equilibrium density  $\rho_0$  and binding energy  $e_0$  are rather well known, and small variations are not important to our conclusions. We therefore fix

$$\rho_0 \equiv \rho_{B0} = 0.1484 \text{ fm}^{-3} \quad (k_F^0 = 1.30 \text{ fm}^{-1}) , \quad (9)$$

$$e_0 \equiv \frac{\mathcal{E}_0}{\rho_0} - M = -16.1 \text{ MeV} = -a_1 . \quad (10)$$

We choose the ranges of acceptable  $K_0$  and  $M_0^*$  based on models that have been directly optimized for finite-nucleus observables, allowing considerable uncertainties. Specifically, we consider

$$180 \text{ MeV} < K_0 < 360 \text{ MeV} , \quad (11)$$

$$0.58 < M_0^*/M < 0.64 . \quad (12)$$

If one focuses on a subset of the nuclear observables, one can stray outside these bounds and still obtain good results. For example, the original Walecka model generates quite acceptable nuclear densities despite its high compression modulus, which yields unfavorable energy systematics [19].

### III. CONSTRAINING NUCLEAR MATTER ENERGY FUNCTIONALS

Given the conditions on the energy functional for nuclear matter [namely,  $e_0$ ,  $\rho_0$ ,  $K_0$ , and  $M_0^*$  in Eqs. (9)–(12)], our goal is to solve for the parameters of the functional as functions of these input “observables.” In general, we can determine four of the parameters from these four inputs, and the additional coefficients will then specify the space of acceptable models. To rule out a class of models, as we will do in Sec. IV, we must show that it is impossible to find a set of coefficients that fall within the bounds of acceptability.

In uniform nuclear matter, the energy functional of Eq. (1) simplifies to the energy density function

$$\begin{aligned} \mathcal{E}(\phi, V_0; \rho_B) = & g_v V_0 \rho_B - \frac{1}{2} m_v^2 V_0^2 + g_v^2 V_0^2 \left( \alpha \frac{M}{g_s} \phi - \frac{1}{2} \alpha' \phi^2 \right) - \frac{1}{4!} \zeta g_v^4 V_0^4 \\ & + \frac{1}{2} m_s^2 \phi^2 + \frac{\kappa}{6} \phi^3 + \frac{\lambda}{24} \phi^4 + \frac{\gamma}{(2\pi)^3} \int^{k_F} d^3 p (\mathbf{p}^2 + M^{*2})^{1/2} , \end{aligned} \quad (13)$$

where

$$M^* \equiv M - g_s \phi , \quad (14)$$

and the Fermi momentum is defined through

$$\rho_B \equiv \frac{\gamma k_F^3}{6\pi^2} . \quad (15)$$

The spin-isospin degeneracy  $\gamma$  is 4 for symmetric nuclear matter. The coefficients  $\kappa$  and  $\lambda$  may be constrained by chiral symmetry (as in the linear sigma model), but are free at this point. Note also, that if we choose to work with a renormalizable lagrangian and include the one-baryon-loop vacuum energy  $\Delta\mathcal{E}_{\text{vac}}$  (either chirally or not), this is equivalent to redefining  $\kappa$  and  $\lambda$  as well as the coefficients of higher powers of  $\phi$  (which are not shown). As before, the parameters and their special values in particular models are given in Table I.

It is useful to change variables in the energy density. First we switch from  $\phi$  and  $V_0$  to the mean-field nucleon self-energies (or optical potentials)  $\Phi$  and  $W$  (following the notation of Ref. [18]):

$$\Phi \equiv g_s \phi , \quad W \equiv g_v V_0 . \quad (16)$$

The meson field equations are now determined by extremizing  $\mathcal{E}$  with respect to  $\Phi$  and  $W$ . As discussed earlier, the natural expansion parameters for the finite-density functional are  $W/M$  and  $\Phi/M$ . The quadratic terms in Eq. (13) imply that the couplings  $g_s$  and  $g_v$  do not appear individually in nuclear matter, so we rewrite the energy density in terms of variables that absorb the couplings. We introduce the ratios of meson couplings to masses

$$c_s \equiv \frac{g_s}{m_s} , \quad c_v \equiv \frac{g_v}{m_v} , \quad (17)$$

together with the scalar self-couplings

$$\bar{\kappa} \equiv \frac{\kappa}{g_s^3} , \quad \bar{\lambda} \equiv \frac{\lambda}{g_s^4} , \quad (18)$$

and the scalar–vector couplings

$$\bar{\alpha} \equiv \frac{\alpha}{g_s^2} , \quad \bar{\alpha}' \equiv \frac{\alpha'}{g_s^2} . \quad (19)$$

The correspondences between conventional model parameters and the newly defined parameters are summarized in Table II. The nucleon mass  $M = 939 \text{ MeV}$  and the vector meson mass  $m_v = m_\omega = 783 \text{ MeV}$  will be fixed at their experimental values.

In terms of the new variables, the energy density can be written as

$$\mathcal{E}(\Phi, W; \rho_B) = \mathcal{E}_{\text{v}\Phi}(\Phi, W; \rho_B) + U(\Phi) + \mathcal{E}_k(\Phi; \rho_B) , \quad (20)$$

where

TABLE II. Relationship between parameters of Eq. (13) and specific models. The quadratic coupling is  $c_s = g_s/m_s$ . Chiral models with a linear representation should have  $g_s = g_\pi$  at the level considered here; however, we will allow  $g_s = g_\pi/g_A$  with  $g_\pi \approx 13.5$  and  $g_A \approx 1.26$ , so that the Goldberger–Treiman relation is satisfied. We have also taken  $m_\pi = 0$  in writing the entries. Recall that the  $\eta$ 's in the last two rows are unrelated.

Model	Ref.	$c_v$	$\bar{\kappa}$	$\bar{\lambda}$	$\zeta$	$\bar{\alpha}$	$\bar{\alpha}'$
Walecka	[44]	$\frac{g_v}{m_v}$	0	0	0	0	0
Nonlinear scalar	[41]	$\frac{g_v}{m_v}$	$-\frac{2b}{g_s^3}$	$\frac{6c}{g_s^4}$	0	0	0
Bodmer	[18]	$\frac{g_v}{m_v}$	$\frac{2a}{g_s^3}$	$\frac{6b}{g_s^4}$	$\frac{6m_v^2}{Z^2 g_v^2}$	0	0
Chiral $\sigma\omega$	[20]	$\frac{g_v}{m_v}$	$-\frac{3}{c_s^2 M}$	$\frac{3}{c_s^2 M^2}$	0	0	0
Boguta	[9]	$\frac{g_s}{M}$	$-\frac{3}{c_s^2 M}$	$\frac{3}{c_s^2 M^2}$	0	$\frac{1}{g_s^2}$	$\frac{1}{g_s^2}$
General chiral	[17]	$\frac{g_v}{m_v}$	$-\frac{3}{c_s^2 M}$	$\frac{3}{c_s^2 M^2}$	$\zeta$	$\frac{\eta}{g_s^2}$	$\frac{\eta}{g_s^2}$
Nonlinear chiral	[36]	$\frac{g_v}{m_v}$	$\frac{(3d-8)}{d(g_s S_0)c_s^2}$	$\frac{(11d^2-48d+48)}{(dg_s S_0)^2 c_s^2}$	$\zeta$	$\frac{-\eta}{2(g_s S_0)c_v^2 M}$	0

$$\mathcal{E}_{v\Phi}(\Phi, W; \rho_B) = W\rho_B - \frac{1}{2c_v^2}W^2 + W^2\left(\bar{\alpha}M\Phi - \frac{1}{2}\bar{\alpha}'\Phi^2\right) - \frac{\zeta}{24}W^4, \quad (21)$$

$$U(\Phi) = \frac{1}{2c_s^2}\Phi^2 + \frac{\bar{\kappa}}{6}\Phi^3 + \frac{\bar{\lambda}}{24}\Phi^4, \quad (22)$$

and  $\mathcal{E}_k$  is the “kinetic energy” (including the nucleon rest mass):

$$\begin{aligned} \mathcal{E}_k(\Phi; \rho_B) &= \frac{\gamma}{(2\pi)^3} \int^{k_F} d^3p \sqrt{\mathbf{p}^2 + M^{*2}} \\ &= \frac{\gamma}{8\pi^2} \left[ k_F E_F^{*3} - \frac{1}{2}M^{*2}k_F E_F^* - \frac{1}{2}M^{*4} \ln\left(\frac{k_F + E_F^*}{M^*}\right) \right], \end{aligned} \quad (23)$$

with

$$E_F^* \equiv \sqrt{k_F^2 + M^{*2}}. \quad (24)$$

This division is useful because it isolates the  $W$  dependence and the parameters in  $U$  ( $c_s^2$ ,  $\bar{\kappa}$ , and  $\bar{\lambda}$ ), for which we will solve. We could also solve for a different set, as in Sec. IV.

The energy per particle ( $\mathcal{E}/\rho_B - M$ ) and pressure  $p$  are determined by the seven free parameters  $c_v$ ,  $c_s$ ,  $\bar{\kappa}$ ,  $\bar{\lambda}$ ,  $\bar{\alpha}$ ,  $\bar{\alpha}'$ , and  $\zeta$ . Any two models with the same values of these constants will give identical results for nuclear matter, so these are the relevant parameters for testing our constraints, rather than those in the original energy functional.

Let us summarize the conditions on  $\mathcal{E}$  as a function of  $\Phi$ ,  $W$ , and  $\rho_B$  [18]. By evaluating these conditions at equilibrium, we will be able to solve for the parameters in terms of the input data  $e_0$ ,  $\rho_0$ ,  $K_0$ , and  $M_0^*$ . We observe immediately that if  $M_0^*$  is given, then  $\Phi_0$  follows trivially from



$$\Phi_0 = M - M_0^* . \quad (25)$$

It is therefore convenient to define the equilibrium values

$$U_0 \equiv U(\Phi_0) = \frac{1}{2c_s^2}\Phi_0^2 + \frac{\bar{\kappa}}{6}\Phi_0^3 + \frac{\bar{\lambda}}{24}\Phi_0^4 , \quad (26)$$

$$U'_0 \equiv U'(\Phi_0) = \left. \frac{dU(\Phi)}{d\Phi} \right|_{\Phi_0} = \frac{1}{c_s^2}\Phi_0 + \frac{\bar{\kappa}}{2}\Phi_0^2 + \frac{\bar{\lambda}}{6}\Phi_0^3 , \quad (27)$$

and

$$U''_0 \equiv U''(\Phi_0) = \left. \frac{d^2U(\Phi)}{d\Phi^2} \right|_{\Phi_0} = \frac{1}{c_s^2} + \bar{\kappa}\Phi_0 + \frac{\bar{\lambda}}{2}\Phi_0^2 . \quad (28)$$

The conditions on  $\mathcal{E}$  are as follows:

1. At any density  $\rho_B$ ,  $\mathcal{E}$  is stationary with respect to  $\Phi$ :

$$\left( \frac{\partial \mathcal{E}}{\partial \Phi} \right)_{W, \rho_B} = 0 . \quad (29)$$

Carrying out this derivative on Eq. (20) and evaluating the result at equilibrium yields

$$\rho_{s0} - W_0^2[\bar{\alpha}M - \bar{\alpha}'\Phi_0] - U'_0 = 0 , \quad (30)$$

where

$$\rho_{s0} \equiv \rho_s(\Phi_0, \rho_0) , \quad (31)$$

with

$$\begin{aligned} \rho_s(\Phi, \rho_B) &= - \left( \frac{\partial \mathcal{E}_k}{\partial \Phi} \right)_{W, \rho_B} = \frac{\gamma}{(2\pi)^3} \int^{k_F} d^3p \frac{M^*}{\sqrt{\mathbf{p}^2 + M^{*2}}} \\ &= \frac{\gamma M^*}{4\pi^2} \left[ k_F E_F^* - M^{*2} \ln \left( \frac{k_F + E_F^*}{M^*} \right) \right] . \end{aligned} \quad (32)$$

2. The vector field appears only in  $\mathcal{E}_{v\Phi}$  and is determined by the equation of constraint

$$\left( \frac{\partial \mathcal{E}}{\partial W} \right)_{\Phi, \rho_B} = \left( \frac{\partial \mathcal{E}_{v\Phi}}{\partial W} \right)_{\Phi, \rho_B} = 0 , \quad (33)$$

which produces (at equilibrium)

$$\rho_0 - \frac{1}{c_v^2}W_0 + W_0[2\bar{\alpha}M\Phi_0 - \bar{\alpha}'\Phi_0^2] - \frac{\zeta}{6}W_0^3 = 0 . \quad (34)$$

3. The binding energy per particle at  $\rho_B = \rho_0$  is  $-e_0$ , so

$$\mathcal{E}_0 = (e_0 + M)\rho_0 . \quad (35)$$

4. The Hugenholtz–van Hove theorem follows by calculating the chemical potential  $\mu$  from  $\mathcal{E}$  in Eq. (20):

$$\mu = \frac{d\mathcal{E}}{d\rho_B} = W + \left( \frac{\partial \mathcal{E}_k}{\partial \rho_B} \right)_{\Phi} = W + \sqrt{k_F^2 + M^{*2}} . \quad (36)$$

Note that we need only take  $(\partial \mathcal{E} / \partial \rho_B)_{\Phi, W}$  to obtain this result, since  $\mathcal{E}$  is stationary with respect to  $\Phi$  and  $W$  from Eqs. (29) and (33). The mean-field energy density is thermodynamically consistent, so the pressure follows from the first law of thermodynamics (as can be explicitly verified by taking derivatives):

$$p = -\mathcal{E} + \rho_B \mu = -\mathcal{E} + \rho_B W + \rho_B E_F^* . \quad (37)$$

The condition for equilibrium is  $p = 0$  at  $\rho_B \neq 0$ , so combining Eq. (35) with Eq. (37) evaluated at equilibrium yields

$$W_0 = e_0 + M - \sqrt{(k_{F0})^2 + M_0^{*2}} . \quad (38)$$

This quite general result provides a direct connection between  $W_0$  and the inputs  $e_0$ ,  $\rho_0$ , and  $M_0^*$  [41,18].

5. The compression modulus  $K$  follows from

$$\frac{1}{9}K(\rho_B) \equiv \rho_B^2 \frac{d^2(\mathcal{E}/\rho_B)}{d\rho_B^2} = \rho_B \frac{d^2 \mathcal{E}}{d\rho_B^2} - 2 \frac{p}{\rho_B} , \quad (39)$$

so that at equilibrium we have

$$\begin{aligned} K_0 \equiv K(\rho_0) &= 9\rho_0 \left. \frac{d^2 \mathcal{E}}{d\rho_B^2} \right|_{\rho_0} \\ &= 9\rho_0 \left[ \frac{\pi^2}{2k_{F0} E_{F0}^*} + \left. \frac{\partial W}{\partial \rho_B} \right|_{\Phi_0, \rho_0} + \left( \left. \frac{\partial W}{\partial \Phi} \right|_{\Phi_0, \rho_0} - \frac{M_0^*}{E_{F0}^*} \right) \left. \frac{d\Phi}{d\rho_B} \right|_{\rho_0} \right] . \end{aligned} \quad (40)$$

Carrying out the derivatives using the field equations<sup>10</sup> produces

$$K_0 = 9\rho_0 \left[ \frac{\pi^2}{2k_{F0} E_{F0}^*} + v_0 - \frac{\left( \frac{M_0^*}{E_{F0}^*} - v_0 l_0 \right)^2}{U_0'' - \rho_{s0}' + l_0^2 v_0 - \bar{\alpha}' W_0^2} \right] , \quad (41)$$

---

<sup>10</sup>This is most simply done by considering  $W$  to be a function of  $\Phi$  and  $\rho_B$ .

where

$$l_0 \equiv \frac{2}{W_0}(\rho_{s0} - U'_0) = 2W_0(\bar{\alpha}M - \bar{\alpha}'\Phi_0) , \quad (42)$$

$$v_0 \equiv \frac{W_0}{\rho_0 + \frac{1}{3}\zeta W_0^3} = \frac{1}{1/c_v^2 - (2\bar{\alpha}\Phi_0 M - \bar{\alpha}'\Phi_0^2) + \frac{1}{2}\zeta W_0^2} , \quad (43)$$

and

$$\rho'_{s0} \equiv \left. \frac{\partial \rho_s}{\partial \Phi} \right|_{\Phi_0} = - \left. \frac{\partial \rho_s}{\partial M^*} \right|_{M_0^*} , \quad (44)$$

with

$$\frac{\partial \rho_s}{\partial M^*} = \frac{\rho_s}{M^*} + \frac{2}{\pi^2} M^{*2} \left[ \frac{k_F}{E_F^*} - \ln \left( \frac{k_F + E_F^*}{M^*} \right) \right] . \quad (45)$$

We can now systematically solve for  $c_v^2$  and the three parameters in  $U(\Phi)$  using the four inputs  $e_0$ ,  $\rho_0$ ,  $K_0$ , and  $M_0^*$ . This leaves as free parameters  $\zeta$ ,  $\bar{\alpha}$ , and  $\bar{\alpha}'$ , which label potentially viable solutions. We note immediately that  $M_0^*$  gives us  $\Phi_0$  from Eq. (25) and then  $W_0$  from Eq. (38). We can now solve Eq. (34) for  $c_v^2$ , since given  $\zeta$ ,  $\bar{\alpha}$ , and  $\bar{\alpha}'$ , everything else is known:

$$c_v^2 = \frac{W_0}{\rho_0 + W_0[2\bar{\alpha}M\Phi_0 - \bar{\alpha}'\Phi_0^2] - \frac{1}{6}\zeta W_0^3} . \quad (46)$$

Next, we express  $c_s^2$ ,  $\bar{\kappa}$ , and  $\bar{\lambda}$  in terms of  $U_0$ ,  $U'_0$ , and  $U''_0$  by inverting Eqs. (26)–(28):<sup>11</sup>

$$c_s^2 = \frac{\frac{1}{2}\Phi_0^2}{\frac{1}{2}\Phi_0^2 U''_0 - 3\Phi_0 U'_0 + 6U_0} , \quad (47)$$

$$\bar{\kappa} = \frac{-\Phi_0^2 U''_0 + 5\Phi_0 U'_0 - 8U_0}{\frac{1}{6}\Phi_0^3} , \quad (48)$$

$$\bar{\lambda} = \frac{\frac{1}{2}\Phi_0^2 U''_0 - 2\Phi_0 U'_0 + 3U_0}{\frac{1}{24}\Phi_0^4} . \quad (49)$$

The final step is to relate  $U_0$ ,  $U'_0$ , and  $U''_0$  to the input observables. After determining  $\Phi_0$ ,  $W_0$ , and  $c_v$ , we can calculate  $\mathcal{E}_{v\Phi}$  and  $\mathcal{E}_k$  at equilibrium. Then  $U_0 \equiv U(\Phi_0)$  follows from Eqs. (20) and (10):

---

<sup>11</sup>At this stage, the form of  $U(\Phi)$  is not critical, and if  $U(\Phi)$  has three unknown parameters (but not necessarily a quartic polynomial), one can just calculate  $U_0$ ,  $U'_0$ , and  $U''_0$  and invert to find the parameters in terms of  $\rho_0$ ,  $e_0$ ,  $M_0^*$ , and  $K_0$  [18].

$$\begin{aligned}
U_0 &= \mathcal{E}_0 - \mathcal{E}_{v\Phi}(\Phi_0, W_0; \rho_0) - \mathcal{E}_k(\Phi_0; \rho_0) \\
&= (e_0 + M)\rho_0 - \mathcal{E}_{v\Phi}(\Phi_0, W_0; \rho_0) - \mathcal{E}_k(\Phi_0; \rho_0) .
\end{aligned} \tag{50}$$

Here  $e_0$ ,  $\rho_0$ ,  $M_0^*$ , and  $\zeta$  are given,  $\mathcal{E}_k(\Phi_0; \rho_0)$  follows from Eq. (23) at the given  $\rho_0$  and  $M_0^*$ , and we use Eqs. (21) and (34) to get  $\mathcal{E}_{v\Phi}(\Phi_0, W_0; \rho_0)$ , with the result

$$\mathcal{E}_{v\Phi}(\Phi_0, W_0; \rho_0) = \frac{1}{2}W_0\rho_0 + \frac{1}{24}\zeta W_0^4 . \tag{51}$$

We can evaluate  $U'_0$  using Eqs. (30) and (32):

$$U'_0 = \rho_{s0} - W_0^2[\bar{\alpha}M - \bar{\alpha}'\Phi_0] \tag{52}$$

and then solve the  $K_0$  equation (41) for  $U''_0$  in terms of known quantities:

$$U''_0 = \rho'_{s0} - l_0^2 v_0 + \bar{\alpha}' W_0^2 + \frac{\left(\frac{M_0^*}{E_{F0}^*} - v_0 l_0\right)^2}{\frac{\pi^2}{2k_{F0}E_{F0}^*} + v_0 - \frac{K_0}{9\rho_0}} . \tag{53}$$

If we use all four inputs  $e_0$ ,  $\rho_0$ ,  $M_0^*$ , and  $K_0$  to determine the parameters  $c_v^2$ ,  $c_s^2$ ,  $\bar{\kappa}$ , and  $\bar{\lambda}$ , we can find solutions parametrized by the remaining free couplings, which are  $\zeta$ ,  $\bar{\alpha}$ , and  $\bar{\alpha}'$  in the general case. It would seem that we can always find a solution. How, then, can we ever exclude a model? There are several possibilities. First, the model may be less general, so that there are not enough free parameters. For example, the Walecka model has only two free parameters ( $c_s^2$  and  $c_v^2$ ); thus, only  $e_0$  and  $\rho_0$  can be specified, and  $M_0^*$  and  $K_0$  are predicted. There is a transcendental equation for  $M_0^*$  to be solved in this case [see Eq. (55), below], and the solution may not fall within the bounds specified by Eq. (12). Another possibility is that the solution manifests unphysical conditions (*e.g.*,  $c_s^2 < 0$  or  $c_v^2 < 0$ ).

A third possibility is that the parameters allow multiple solutions to the meson field equations, which may correspond to pathological or abnormal solutions (*e.g.*, a Lee–Wick solution [4] in the sigma model). These alternative solutions extremize the energy functional and may have a lower energy than the normal solution (which satisfies the phenomenological input conditions). As discussed in the next section, we will not necessarily exclude a model in this case unless the normal solution, which exists by construction at  $\rho_0$ , disappears at a slightly higher density. If this occurs, we must consider the parameter set unacceptable.

To investigate the latter possibility, we must always check for multiple solutions to the  $\Phi$  and  $W$  equations [(30) and (34)] after determining the parameters. Equation (34) is easy to analyze, since it is a cubic in  $W$  with known coefficients (for given  $\Phi$ ). For example, one can show that with  $\bar{\alpha} = \bar{\alpha}' = 0$ , it is necessary that  $\zeta > 0$  to avoid abnormal nuclear matter solutions with lower energy than the normal solution. We illustrate what can happen with multiple solutions in Fig. 1, for  $\bar{\alpha} = \bar{\alpha}' = 0$  and  $\zeta = -0.03$ . The solid line is the normal solution, with a minimum at  $e_0$  and  $\rho_0$ . The other curves arise from different solutions to the  $W$  and  $\Phi$  equations (three each!). The normal solution disappears at a density slightly above  $\rho_0$ , and only pathological solutions remain at higher densities (not shown).

A final possibility is that the parameter set is unnatural, that is, the coefficients of the highest-order terms are too large. These terms then dominate the energy functional at

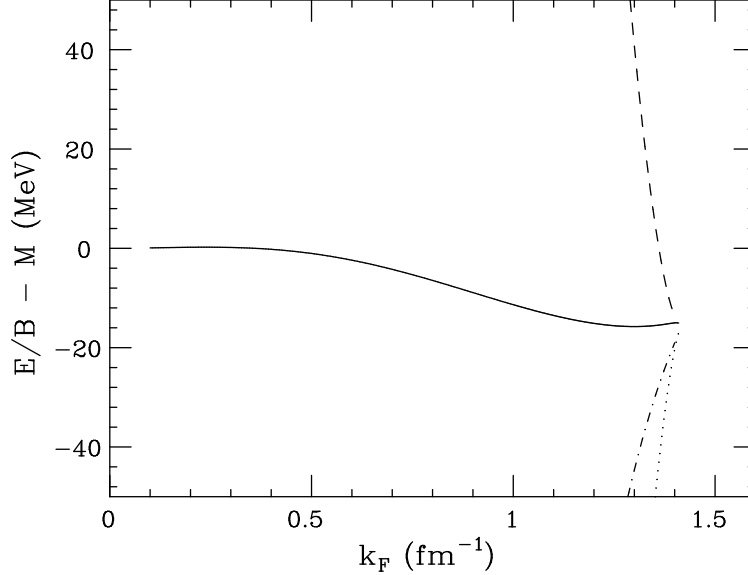


FIG. 1. Binding-energy curves with  $\zeta = -0.03$ ,  $\bar{\alpha} = \bar{\alpha}' = 0$ , and all other parameters determined from  $e_0$ ,  $\rho_0$ ,  $M_0^*$ , and  $K_0$ . All of the curves extremize the energy functional. The normal solution (with equilibrium binding energy  $-16.1$  MeV at  $k_F = 1.3$   $\text{fm}^{-1}$ ) is the solid line. Only four of the six solutions are shown.

densities near nuclear matter equilibrium, which implies that our truncation is unjustified, and the entire framework breaks down.

The Bodmer method for determining the model parameters from information about nuclear matter equilibrium can be conveniently implemented in a spreadsheet or symbolic manipulation program. It can be summarized as follows:

1. Specify  $e_0$ ,  $\rho_0$ ,  $K_0$ ,  $M_0^*$ , and also  $\zeta$ ,  $\bar{\alpha}$ , and  $\bar{\alpha}'$ . (Here we have chosen to solve for  $c_v^2$ ,  $c_s^2$ ,  $\bar{\kappa}$ , and  $\bar{\lambda}$ .)
2.  $\Phi_0$  follows from Eq. (25) and  $W_0$  from Eq. (38).
3. Determine  $c_v^2$  from Eq. (46). If  $m_v$  is specified, then  $g_v^2$  follows immediately from the definition in Eq. (17).
4. Compute  $U_0$  from Eqs. (50), (51), and (23);  $U_0'$  from Eqs. (32) and (52); and  $U_0''$  from Eqs. (42)–(45) and (53). Solve for  $c_s^2$ ,  $\bar{\kappa}$ , and  $\bar{\lambda}$  from Eqs. (47)–(49). If the scalar mass  $m_s$  is also specified, one can obtain  $g_s$ ,  $\kappa$ , and  $\lambda$  from Eqs. (17) and (18).
5. Find all solutions to the scalar and vector equations. (It is easiest to first eliminate  $W$  from the  $\Phi$  equation by directly solving the cubic  $W$  equation.) Check that the normal solution is acceptable within a prescribed density range.

As a starting point for our discussion, we set  $\bar{\alpha} = \bar{\alpha}' = 0$ , so that we consider the same class of models studied by Bodmer [18]. A useful procedure is to fix  $e_0$  and  $\rho_0$  and then to scan the  $(K_0, M_0^*)$  plane, with each point producing a family of parameter sets, since

there are five free parameters and only four constraints. We can then establish boundaries corresponding to special values of the parameters.

With  $\bar{\alpha} = \bar{\alpha}' = 0$ , the energy density reduces to

$$\mathcal{E} = W\rho_{\text{B}} + \mathcal{E}_k(\Phi; \rho_{\text{B}}) - \frac{1}{2c_{\text{v}}^2}W^2 + \frac{1}{2c_{\text{s}}^2}\Phi^2 + \frac{1}{6}\bar{\kappa}\Phi^3 + \frac{1}{24}\bar{\lambda}\Phi^4 - \frac{1}{24}\zeta W^4. \quad (54)$$

This implies that

- $\zeta > 0$  lowers the energy (attractive),
- $\bar{\kappa}, \bar{\lambda} > 0$  raise the energy (repulsive),
- $\bar{\kappa}, \bar{\lambda} < 0$  lower the energy (attractive).

If  $\bar{\kappa} = \bar{\lambda} = 0$  (no scalar nonlinearities) and  $\zeta = 0$  (no vector nonlinearities), then we obtain the original Walecka model. In equilibrium, we can set  $\mathcal{E}$  from Eq. (54) equal to  $(e_0 + M)\rho_0$ , and eliminate  $W_0$  using Eq. (38),  $c_{\text{s}}^2$  using Eq. (30), and  $c_{\text{v}}^2$  using Eq. (34). This leaves a transcendental equation for  $M_0^*$ :

$$(e_0 + M)\rho_0 + \sqrt{(k_{\text{F}0})^2 + M_0^{*2}}\rho_0 - (M - M_0^*)\rho_{\text{s}0} - 2\mathcal{E}_k(M_0^*; \rho_0) = 0. \quad (55)$$

For the values of  $\rho_0$  and  $e_0$  in Eqs. (9) and (10), the solution is  $M_0^*/M = 0.538$ , which then implies  $K_0 = 557$  MeV from Eq. (41). This point is denoted as (A) in Fig. 2.

If  $\zeta = 0$  but  $\bar{\kappa} \neq 0$  and  $\bar{\lambda} \neq 0$ , it is possible to reproduce the desired  $M_0^*$  and  $K_0$  with  $U(\Phi)$  alone, which is well known. In this case,  $\bar{\kappa} > 0$  and  $\bar{\lambda} < 0$ . The situation can be displayed graphically in the following figures. In Fig. 2, we plot the locus of points for which  $\bar{\kappa} = 0$  or  $\bar{\lambda} = 0$ , as a function of both  $M_0^*/M$  and  $K_0$ . This lets us separate the regions of parameter space corresponding to different signs of  $\bar{\kappa}$  and  $\bar{\lambda}$ . The boxed area shows the acceptable values of the input ‘‘observables’’ ( $0.58 \leq M_0^*/M \leq 0.64$ ,  $180 \leq K_0 \leq 360$  MeV). Note that when  $\bar{\lambda} < 0$ , the energy is unbounded below for large  $\Phi$ ; this is not necessarily a problem, however, since our truncated functional is only valid for small  $\Phi$ .

If we now allow  $\zeta \neq 0$  (recall that  $\zeta$  must be positive), then as  $\zeta$  increases, we get additional attractive contributions to the energy, which leads us to increase  $\bar{\lambda}$ . Figure 3 shows lines of  $\bar{\lambda} = 0$  for selected values of  $c_{\text{v}}^2\zeta W_0^2/6$ . [This combination is the ratio of the cubic and linear terms in Eq. (34) and is thus the relevant measure of vector nonlinearities.] For large enough  $\zeta$ , we can achieve acceptable  $M_0^*$  and  $K_0$  with  $\bar{\lambda} > 0$ . We can see how this works by examining the expression for  $\mathcal{E}$  in Eq. (54). Since both  $\Phi_0$  and  $W_0$  are approximately proportional to  $\rho_{\text{B}}$ , a phenomenologically acceptable  $\mathcal{E}$  clearly requires an explicit dependence  $\propto \rho_{\text{B}}^4$  with a negative coefficient. If  $\zeta = 0$ , we must set  $\bar{\lambda} < 0$  to achieve this. By setting  $\zeta > 0$ , however, we can increase  $\bar{\lambda}$  and obtain essentially the same result. Nevertheless, we must be careful not to let the quartic nonlinearities get so large that they dominate the energy, for this would violate our assumption of naturalness.

If we hold  $\bar{\kappa} = \bar{\lambda} = \bar{\alpha} = \bar{\alpha}' = 0$  and let  $\zeta > 0$  (vector nonlinearities only), then  $M_0^*/M$  decreases and  $K_0$  increases relative to the Walecka model, as indicated by the line in Fig. 4. Thus adding  $\zeta$  alone makes the resulting nuclear matter properties worse; to return to the desired region of  $M_0^*$  and  $K_0$ , we must restore the scalar nonlinearities. Furthermore, when

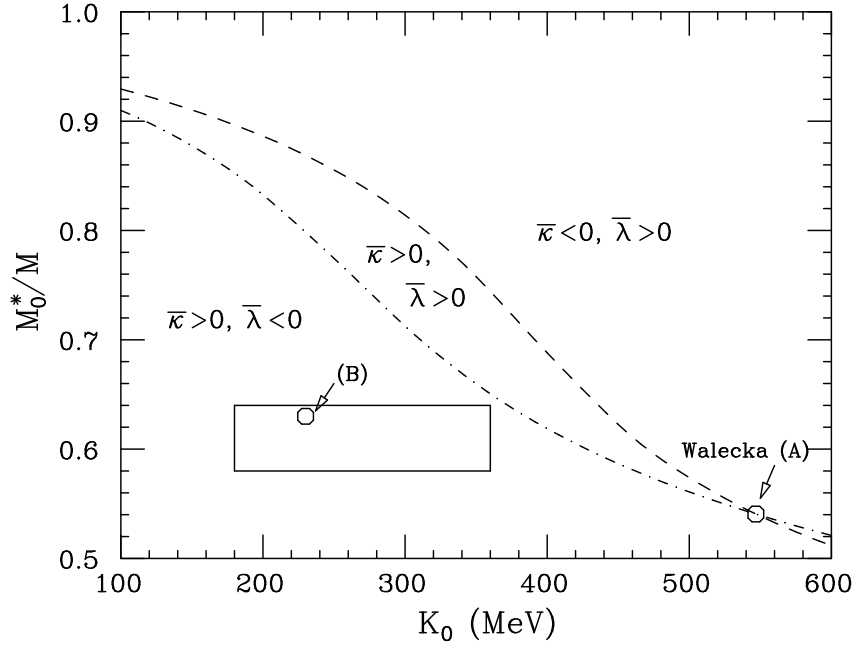


FIG. 2.  $M_0^*/M$  vs.  $K_0$  with  $\zeta = \bar{\alpha} = \bar{\alpha}' = 0$ . The lines show the  $\bar{\kappa} = 0$  and  $\bar{\lambda} = 0$  boundaries. The box encloses the desirable values of  $M_0^*/M$  and  $K_0$ . Model B is from Ref. [17] (see Table III).

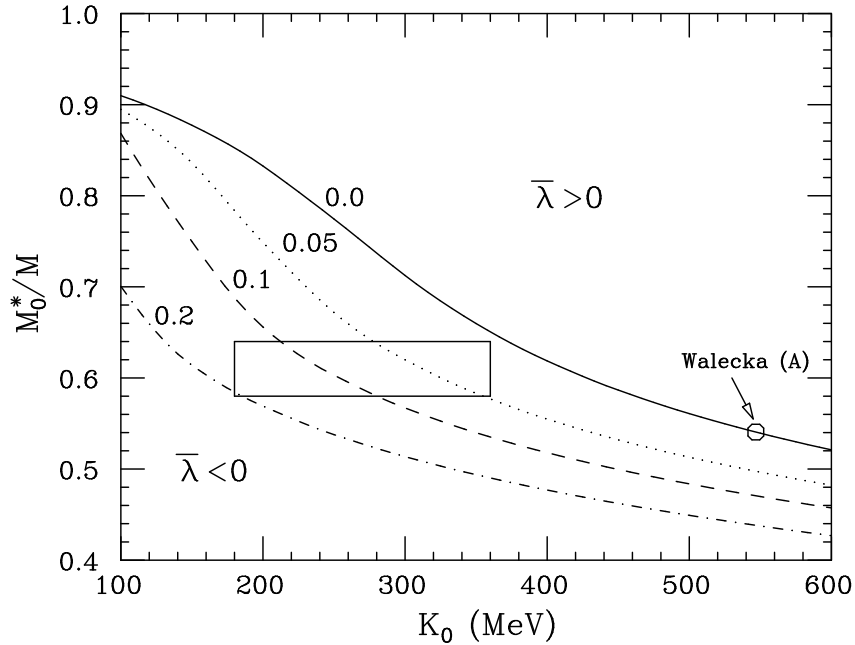


FIG. 3.  $M_0^*/M$  vs.  $K_0$  with  $\bar{\alpha} = \bar{\alpha}' = 0$ . The lines show the  $\bar{\lambda} = 0$  boundaries for a range of values of  $c_v^2 \zeta W_0^2 / 6$  from 0.0 to 0.2. This combination is a measure of the vector nonlinearities. The box encloses the desirable values of  $M_0^*/M$  and  $K_0$ .

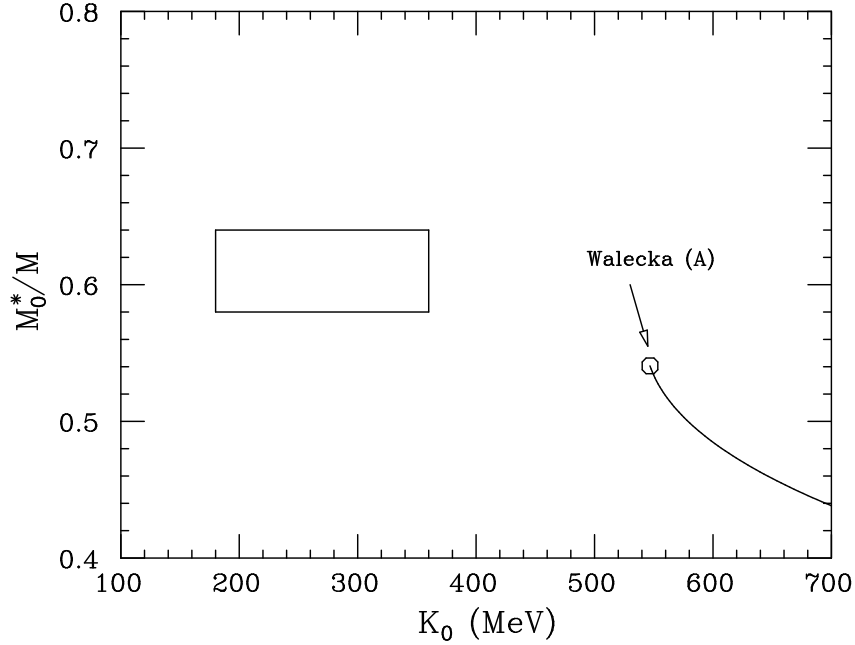


FIG. 4.  $M_0^*/M$  vs.  $K_0$  with  $\bar{\alpha} = \bar{\alpha}' = 0$  and  $\bar{\kappa} = \bar{\lambda} = 0$ . The line shows possible solutions as a function of  $\zeta c_V^2 W_0^2/6$ . The  $\zeta = 0$  point is the Walecka model. The box encloses the desirable values of  $M_0^*/M$  and  $K_0$ .

one increases  $\zeta$ , one must compensate by increasing  $\lambda$ , so that an acceptable description is obtained only when both terms are included. This conclusion is consistent with our definition of naturalness and is also supported by the density dependence of the scalar and vector self-energies found in DBHF calculations [42].

One can further explore the space of acceptable parametrizations by letting  $\bar{\alpha} \neq 0$  and  $\bar{\alpha}' \neq 0$ . Although the enlarged parameter space allows for a wide variety of acceptable solutions, this additional freedom is not needed to satisfy the phenomenological constraints considered here. Nevertheless, two observations can be made. First, including the  $\bar{\alpha}$  and  $\bar{\alpha}'$  parameters allows one to adjust the density dependence of the effective scalar and vector meson masses (defined by diagonalizing the matrix of appropriate second derivatives of the energy functional), which may provide useful constraints in the future if concrete empirical information becomes available. (Note that one must be careful of the distinction between longitudinal and transverse masses when trying to compare with experiment.) These additional parameters may also allow for improved fits to DBHF self-energies or to self-energies obtained in more sophisticated nuclear matter calculations. Second, our definition of naturalness says that there is no reason to omit these scalar–vector couplings, unless there is some (as yet unknown) symmetry principle that forbids them. In the interest of brevity, we leave an exploration of the expanded parameter space to a future investigation. We turn instead to specific chiral models, considered as special cases of the full energy functional, and apply a variant of the Bodmer analysis described above.



#### IV. ANALYSIS OF LINEAR SIGMA MODELS

We now adapt the general analysis of the previous section to consider mean-field models built on the linear sigma model with a light scalar meson. There is a long history of such models, starting with the lagrangian considered by Kerman and Miller [5,20]:

$$\begin{aligned} \mathcal{L} = & \bar{\psi}[i\gamma_\mu\partial^\mu - g_v\gamma_\mu V^\mu - g_\pi(\sigma + i\gamma_5\boldsymbol{\tau}\cdot\boldsymbol{\pi})]\psi \\ & + \frac{1}{2}(\partial_\mu\sigma\partial^\mu\sigma + \partial_\mu\boldsymbol{\pi}\cdot\partial^\mu\boldsymbol{\pi}) - \frac{1}{4}\lambda(\sigma^2 + \boldsymbol{\pi}^2 - v^2)^2 \\ & - \frac{1}{4}(\partial_\mu V_\nu - \partial_\nu V_\mu)^2 + \frac{1}{2}m_v^2 V_\mu V^\mu + \epsilon\sigma . \end{aligned} \quad (56)$$

Because of the ‘‘Mexican-hat’’ potential,  $v \neq 0$  implies that  $\sigma$  acquires a nonzero vacuum expectation value, which generates masses for the nucleon and scalar meson (and pion). This also fixes the self-couplings of the scalar field  $\phi$  that is the deviation of  $\sigma$  from its vacuum value. Here we study descriptions of nuclei that arise from generalizations of this model. We stress that we are now exploring the phenomenological consequences of definite lagrangians treated in the Hartree approximation. We are able to use the effective density functional analysis developed in the previous sections because the form of the energy functional is the same.

The general extension of the linear sigma model (56) considered in Ref. [17] is based on the lagrangian (after shifting the scalar field  $\sigma$  from its vacuum value to define  $\phi$ )

$$\begin{aligned} \mathcal{L} = & \bar{\psi}[i\gamma_\mu\partial^\mu - g_v\gamma_\mu V^\mu - (M - g_\pi\phi) - ig_\pi\gamma_5\boldsymbol{\tau}\cdot\boldsymbol{\pi}]\psi \\ & + \frac{1}{2}(\partial_\mu\phi\partial^\mu\phi - m_s^2\phi^2) + \frac{1}{2}(\partial_\mu\boldsymbol{\pi}\cdot\partial^\mu\boldsymbol{\pi} - m_\pi^2\boldsymbol{\pi}^2) \\ & + \frac{g_\pi}{2M}(m_s^2 - m_\pi^2)\phi(\phi^2 + \boldsymbol{\pi}^2) - \frac{g_\pi^2}{8M^2}(m_s^2 - m_\pi^2)(\phi^2 + \boldsymbol{\pi}^2)^2 \\ & - \frac{1}{4}(\partial_\mu V_\nu - \partial_\nu V_\mu)^2 + \frac{1}{2}m_v^2 V_\mu V^\mu + \frac{1}{4!}\zeta g_v^4 (V_\mu V^\mu)^2 \\ & - \eta^2 \left( \frac{g_v^2}{g_\pi} \right) M V_\mu V^\mu \phi + \frac{1}{2}\eta^2 g_v^2 V_\mu V^\mu (\phi^2 + \boldsymbol{\pi}^2) . \end{aligned} \quad (57)$$

Here we have eliminated  $\lambda$ ,  $v$ , and  $\epsilon$  in favor of  $M$ ,  $m_s$ , and  $m_\pi$ . We will take  $m_\pi = 0$  in the sequel.<sup>12</sup> This is the most general lagrangian with nonderivative couplings through dimension four that is consistent with linear chiral symmetry (for  $m_\pi = 0$ ).

---

<sup>12</sup>When solving chiral mean-field models, one must be aware of the possibility of bound ‘‘anomalous’’ solutions, in which the scalar field interpolates between the minima of the effective potential. Including a finite pion mass increases the energy of the anomalous solution so that it is above the energy of the normal solution. Hence we can simply ignore these anomalous solutions and set  $m_\pi = 0$ . (The pion mass has negligible effect on ‘‘normal’’ solutions.)

Note that chiral symmetry in the linear realization implies that the scalar–nucleon Yukawa coupling constant  $g_s$  is equal to the pion–nucleon coupling constant  $g_\pi$ , which is known experimentally. Moreover, the nucleon mass satisfies  $M = g_\pi f_\pi$  at the one-loop level. Since this implies  $g_A = 1$ , in contradiction to experiment, we will allow  $g_s = g_\pi/g_A$  when working at the Hartree level.

In the Hartree approximation, the pion field vanishes for nuclear matter or axially symmetric nuclei, and the energy functional derived from Eq. (57) reduces to a special case of the functional considered earlier. In nuclear matter there are four free parameters:  $c_s^2$ ,  $c_v^2$ ,  $\bar{\alpha} = \bar{\alpha}' = \eta^2/g_s^2$ , and  $\zeta$ . We can adapt the analysis of Sec. III to solve for these parameters in terms of the inputs  $e_0$ ,  $\rho_0$ ,  $K_0$ , and  $M_0^*$ . Naively, this would seem to imply that we *can* find good sigma-model descriptions of finite nuclei, in contrast to the conclusion of Ref. [17]. We first present the analysis and then discuss why this is not the case.

To specialize the general functional of Secs. II and III to the chiral models from Ref. [17], we set [see Eq. (22)]

$$\bar{\alpha}' = \bar{\alpha} = \frac{\eta^2}{g_s^2} > 0 , \quad (58)$$

$$\bar{\kappa} = -\frac{3}{M} \frac{1}{c_s^2} < 0 , \quad (59)$$

$$\bar{\lambda} = \frac{3}{M^2} \frac{1}{c_s^2} > 0 . \quad (60)$$

Now  $\mathcal{E}$  takes the form

$$\begin{aligned} \mathcal{E} = & W\rho_B + \mathcal{E}_k(\Phi; \rho_B) - \frac{1}{2c_s^2}W^2 - \frac{1}{4!}\zeta W^4 \\ & + \frac{1}{2c_s^2}\Phi^2\left(1 - \frac{\Phi}{M} + \frac{\Phi^2}{4M^2}\right) + \frac{1}{2}\bar{\alpha}W^2(M^2 - M^{*2}) . \end{aligned} \quad (61)$$

At equilibrium,  $\Phi_0$  still follows trivially from  $M_0^*$ :

$$\Phi_0 = M - M_0^* , \quad (62)$$

and the scalar potential and its derivatives can be evaluated from Eqs. (26)–(28) using the relations (59) and (60). We can then simply rewrite the equilibrium conditions from Sec. III (as before, a subscript “0” denotes the value at equilibrium):

1. The scalar field equation becomes

$$\rho_{s0} - \bar{\alpha}M_0^*W_0^2 - \frac{1}{c_s^2}\Phi_0\left[1 - \frac{3\Phi_0}{2M} + \frac{\Phi_0^2}{2M^2}\right] = \rho_{s0} - \bar{\alpha}M_0^*W_0^2 - \frac{M_0^*(M^2 - M_0^{*2})}{2c_s^2M^2} = 0 , \quad (63)$$

where  $\rho_s$  is still given by Eq. (32).

2. The vector field constraint equation is

$$\rho_0 - \frac{1}{c_v^2} W_0 + \bar{\alpha} W_0 [M^2 - M_0^{*2}] - \frac{\zeta}{6} W_0^3 = 0 . \quad (64)$$

3. The energy density can be written explicitly as

$$\begin{aligned} \mathcal{E}_0 &= (e_0 + M) \rho_0 \\ &= \frac{1}{2} W_0 \rho_0 + \frac{1}{24} \zeta W_0^4 + \frac{1}{2c_s^2} \Phi_0^2 \left( 1 - \frac{\Phi_0}{M} + \frac{\Phi_0^2}{4M^2} \right) + \mathcal{E}_k(\Phi_0; \rho_0) , \end{aligned} \quad (65)$$

with  $\mathcal{E}_k(\Phi_0; \rho_0)$  evaluated from Eq. (23). The second equality is obtained from Eq. (61) using the equation of constraint (64). Observe that there is no explicit dependence on  $\bar{\alpha}$  in Eq. (65).

4. The Hugenholtz–van Hove theorem goes through as before, and we again find

$$W_0 = e_0 + M - \sqrt{(k_{F0})^2 + M_0^{*2}} . \quad (66)$$

5. The compression modulus at equilibrium is

$$K_0 = 9\rho_0 \left[ \frac{\pi^2}{2k_{F0} E_{F0}^*} + v_0 - \frac{(M_0^*/E_{F0}^* - v_0 l_0)^2}{U_0'' - \rho_{s0}' + l_0^2 v_0 - \bar{\alpha} W_0^2} \right] , \quad (67)$$

with  $\rho_{s0}'$  still evaluated from Eq. (45), but now

$$l_0 = 2\bar{\alpha} M_0^* W_0 , \quad (68)$$

$$v_0 = \frac{W_0}{\rho_0 + \frac{1}{3}\zeta W_0^3} , \quad (69)$$

and

$$U_0'' = \frac{1}{c_s^2} \left[ 1 - 3\frac{\Phi_0}{M} + \frac{3\Phi_0^2}{2M^2} \right] . \quad (70)$$

One can solve Eqs. (62)–(70) for  $c_s^2$ ,  $\bar{\alpha}$ ,  $\zeta$ , and  $c_v^2$  with some straightforward algebra. After eliminating  $\bar{\alpha}$ ,  $\zeta$ , and  $c_v^2$ , the resulting equation involving  $c_s^2$  is actually linear and yields

$$c_s^2 = \frac{\frac{W_0 M_0^{*2}}{M^2} + \frac{M_0^{*2} \zeta_4}{(E_{F0}^*)^2} - \frac{4M_0^* \zeta_5}{E_{F0}^*} - \xi_1 \left( \frac{M_0^{*2}}{M^2} \xi_2 + \xi_3 \xi_4 - \frac{8\rho_{s0}}{W_0} \xi_5 \right)}{\xi_1 \left( \frac{4\rho_{s0}^2}{W_0} - \xi_2 \xi_3 \right) + W_0 \xi_3 - \frac{4M_0^* \rho_{s0}}{E_{F0}^*} + \frac{M_0^{*2}}{(E_{F0}^*)^2} \xi_2} , \quad (71)$$

where

$$\xi_1 \equiv \frac{K_0}{9\rho_0} - \frac{\pi^2}{2k_{\text{F}0}E_{\text{F}0}^*}, \quad (72)$$

$$\xi_2 \equiv \frac{8}{W_0} [(e_0 + M)\rho_0 - \mathcal{E}_{k0}] - 3\rho_0, \quad (73)$$

$$\xi_3 \equiv \rho'_{s0} + \rho_{s0}/M_0^*, \quad (74)$$

$$\xi_4 \equiv \frac{\Phi_0^2}{W_0} \left(1 + \frac{M_0^*}{M}\right)^2, \quad (75)$$

$$\xi_5 \equiv \Phi_0 \left(1 - \frac{3\Phi_0}{2M} + \frac{\Phi_0^2}{2M^2}\right), \quad (76)$$

with  $\mathcal{E}_{k0} \equiv \mathcal{E}_k(\rho_0, M_0^*)$ . The remaining parameters are determined from

$$\bar{\alpha} = \frac{1}{W_0^2 M_0^*} \left[ \rho_{s0} - \frac{1}{c_s^2} \Phi_0 \left(1 - \frac{3\Phi_0}{2M} + \frac{\Phi_0^2}{2M^2}\right) \right], \quad (77)$$

$$\zeta = \frac{24}{W_0^4} \left[ (e_0 + M - \frac{1}{2}W_0)\rho_0 - \mathcal{E}_{k0} - \frac{1}{2c_s^2} \Phi_0^2 \left(1 - \frac{\Phi_0}{M} + \frac{\Phi_0^2}{4M^2}\right) \right], \quad (78)$$

$$c_v^2 = \frac{W_0}{\rho_0 + \bar{\alpha}W_0(M^2 - M_0^{*2}) - \zeta W_0^3/6}. \quad (79)$$

We can use these results to explore the entire range of acceptable normal solutions. The procedure to find parameter sets is direct: specify  $e_0$ ,  $\rho_0$ ,  $M_0^*$ , and  $K_0$ , and the parameters follow algebraically. Nevertheless, the resulting parameter sets will not always be acceptable. For example, parametrizations with  $c_s^2 < 0$  or  $c_v^2 < 0$  are unphysical. In most cases, however, the main issue is the influence of the Lee–Wick solution.

If we recall from Eq. (32) that  $\rho_s \propto M^*$ , it is clear that at any density, Eq. (63) will *always* be satisfied when  $M^* = 0$  or  $\Phi = M$ . This is the Lee–Wick solution, which is an alternative to the “normal” solution, the latter being identified as having zero energy at  $\rho_B = 0$ . (In general, there is also an “anomalous” solution, which arises from a local *maximum* in the energy density as a function of  $M^*$ .) There is no evidence that Lee–Wick states exist in nature. Notwithstanding, while the Lee–Wick solution exists formally at all densities, we are not guaranteed that the normal solution specified at equilibrium will persist at higher density (it may coalesce with the “anomalous” solution and disappear).

An example of the difficulties of bifurcation and coalescence that typically arise from the highly nonlinear field equations is found in the original work of Kerman and Miller [5]. In this  $\sigma\omega$  model [Eq. (61) with  $\bar{\alpha} = \zeta = 0$ ], there are only two free parameters, as in the original Walecka model. Proceeding as in that case (see Sec. III), one discovers that there is *no normal solution* that reproduces the desired  $e_0$  and  $\rho_0$  as an equilibrium point. The best one can do is to satisfy one of the conditions, for example, to reproduce the desired energy/particle  $e_0$  at a density  $\rho_0$ ; however, the system will not be in equilibrium (the pressure is negative), and moreover, the normal solution fails to exist at densities  $\rho > \rho_0$ . This situation is depicted in Fig. 5. Note that the Lee–Wick solution has the lowest energy at most densities and is the only solution at high density.

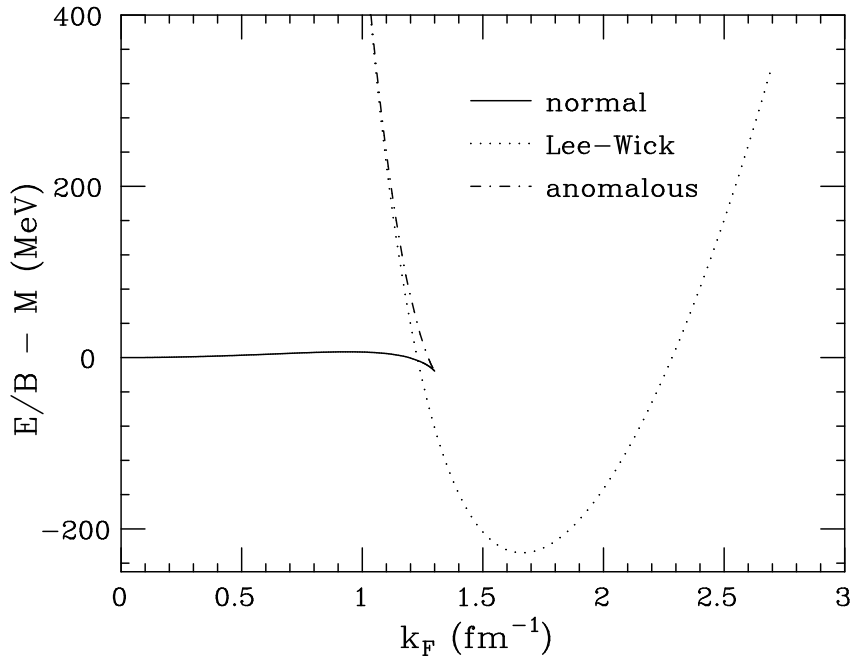


FIG. 5. Nuclear matter binding-energy curves for the simple linear  $\sigma\omega$  model. The normal solution has the standard  $e_0$  at density  $\rho_0$ , but this is not a point of equilibrium.

These results suggest that we might consider a parametrization acceptable only if it produces a normal state with the lowest energy, at least up to the equilibrium density. Alternatively, if one recalls that our energy density is truncated at some finite power of  $\Phi/M$ , one might say that the Lee–Wick solution with  $\Phi = M$  is simply irrelevant. In particular, one could argue that it is possible to add (chirally invariant) repulsive terms of very high order in  $\Phi/M$  that would have negligible effect on the normal solution, but which increase the energy of the Lee–Wick state enough to raise it above the normal state. Rather than digress into a somewhat extraneous discussion about the proper role of the Lee–Wick solution in an effective field theory, we will instead impose on our parameter sets a less restrictive, more physical constraint that is incontrovertible: If a normal solution is found that satisfies the desired inputs, it cannot *disappear* at too low a density to be useful.

To make the consequences of this constraint more concrete, so that we can determine the boundaries of acceptable parametrizations, we will fix  $e_0$  and  $\rho_0$  as usual and then scan the  $(K_0, M_0^*)$  plane, finding the unique normal parameter set ( $c_s^2$ ,  $c_v^2$ ,  $\bar{\alpha}$ , and  $\zeta$ ) at each point. This allows us to determine regions of the plane in which it is impossible to find a normal solution at  $\rho_0$ , in which a normal solution exists at  $\rho_0$  but disappears at some higher density, and in which a normal solution exists at all densities.

The results are summarized in Fig. 6, where some points corresponding to specific models<sup>13</sup> from Tables I and II are indicated. (See Table III for parameter values.) The solid and

<sup>13</sup>These model parameters from Ref. [17] have been adjusted slightly so that nuclear matter

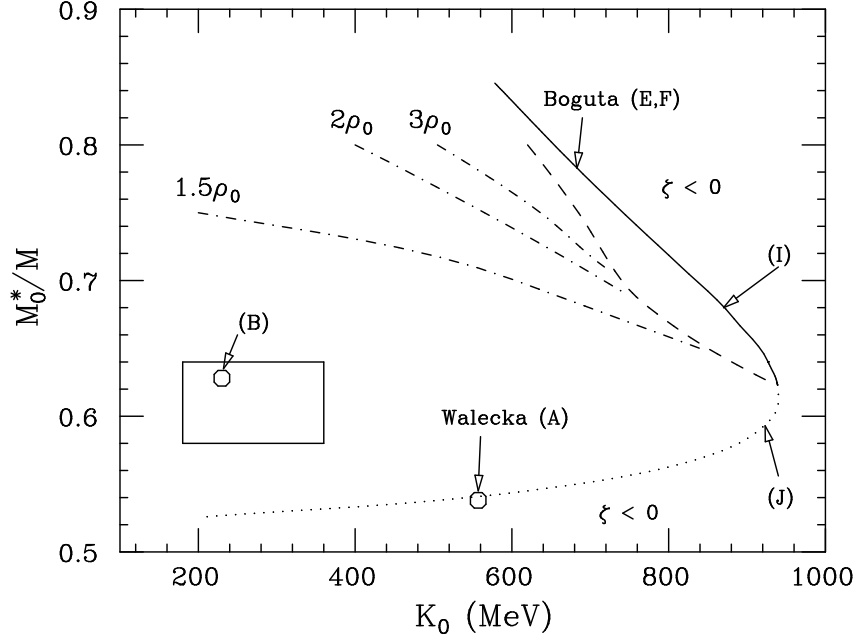


FIG. 6.  $M_0^*/M$  vs.  $K_0$  for generalizations of the conventional linear sigma model. All results have  $e_0 = -16.1 \text{ MeV}$  and  $\rho_0 = 0.1484 \text{ fm}^{-3}$ . The box denotes the desirable region, and the results of some specific parametrizations are indicated by capital letters. The curves are discussed in the text.

dotted curve is the locus of solutions with  $\zeta = 0$ ; on the solid branch, the normal nuclear matter solutions exist at all densities, while on the dotted branch, the normal solutions disappear at  $\rho \leq 1.38\rho_0$ . (There is indeed a discontinuity in the behavior of the solutions.) Regions of the plane to the right and below this curve require  $\zeta < 0$ , which is physically unacceptable, as discussed earlier. The dashed curve marks the boundary where normal solutions with finite  $\zeta$  remain stable at all densities; thus, only in the small region of the plane between the dashed and solid curves can such solutions be found, and this region lies far from the desired one.

The dot-dashed curves are labeled by the value of the density at which the normal solution with the specified inputs disappears. Therefore, while it is technically possible to find parameter sets for inputs lying within the box, the normal solution disappears at much too low a density to be useful. (For example, chiral-model parameters that reproduce the inputs at point *B* generate a normal solution that vanishes at  $\rho = 1.07\rho_0$ .)

Although the choice of limiting density at which the normal state should exist is somewhat subjective, it is reasonable to demand that it persist at least up to  $\rho = 2\rho_0$ , since such densities have clearly been created in the laboratory. As indicated in the figure, enforcing such a constraint makes it impossible to achieve the desired values of  $K_0$  and  $M_0^*$ . The underlying problem is the  $\Phi^3$  coefficient, with its fixed sign and large magnitude [see Eq. (59)], which yields too much attraction. From Fig. 2, we see that  $\bar{\kappa} < 0$  solutions (with

---

saturates at  $e_0 = -16.1 \text{ MeV}$ .

TABLE III. Parameters for the models from Ref. [17] considered in the figures, given in the form of dimensionless ratios as in Eq. (83). All parameter values have been multiplied by  $10^3$  and  $K_0$  is in MeV. The coefficients have been adjusted slightly so that  $e_0 = -16.1$  MeV. All models have  $\zeta = 0$ , and  $\bar{\alpha} = \bar{\alpha}'$ .

Model	$\frac{1}{2c_s^2 M^2}$	$\frac{1}{2c_v^2 M^2}$	$\frac{\bar{\kappa}}{6M}$	$\frac{\bar{\lambda}}{24}$	$\bar{\alpha}$	$M_0^*/M$	$K_0$
A	1.389	1.815	0.0	0.0	0.0	0.54	560
B	1.478	2.309	0.940	-0.900	0.0	0.63	230
E,F	3.499	7.315	-3.499	0.875	14.627	0.78	680
I	2.781	4.654	-2.781	0.695	7.061	0.68	870
J	2.470	3.840	-2.480	0.618	5.406	0.59	920

$\bar{\alpha} = \zeta = 0$ ) correspond to values of  $K_0$  and  $M_0^*$  far from the phenomenologically desirable values. Allowing  $\bar{\alpha} = \bar{\alpha}' > 0$  and  $\zeta > 0$  can produce normal solutions with the desired equilibrium properties, but the consequent nonlinearities are too extreme, and the normal solution disappears at too low a density.

For completeness, we also consider the effect of the one-baryon-loop zero-point energy. This is strictly applicable only with a renormalizable subset of the lagrangians (namely, those with  $\bar{\alpha} = \zeta = 0$ ), but it has been applied more widely in actual calculations [11,17]. The change to the energy density is the addition of

$$\Delta\mathcal{E}_c = \frac{M}{3\pi^2}\Phi^3 - \frac{1}{3\pi^2}\Phi^4 + \Delta\mathcal{E}_{\text{vac}}(M^*), \quad (80)$$

where  $\Delta\mathcal{E}_{\text{vac}}(M^*)$  is the one-loop energy defined in Ref. [20], which starts at  $O(\Phi^5)$  and is numerically unimportant here. Historically, the motivation for adding  $\Delta\mathcal{E}_c$  was to include some repulsion  $\propto \Phi^3$  to cancel the strong attraction in the linear sigma model. It is now possible to find a saturating solution, which exists at all densities (see Fig. 59 in Ref. [20]), but it is far from the favored region, since  $M_0^*/M \approx 0.9$  is much too large. Allowing additional parameters does not change this result.

Of course, the real test of any parameter set comes in its predictions for the properties of finite nuclei. We solve the equations for the finite system using conventional methods [19,22]. For chiral models with a linear realization of the symmetry, we require that  $g_s = g_\pi \approx 13.4$  or<sup>14</sup>  $g_s = g_\pi/g_A$  with  $g_A \approx 1.26$ . Thus, once we establish  $c_s$  from the nuclear matter analysis,  $m_s$  is determined (recall that  $c_s = g_s/m_s$ ). As noted in Ref. [17], this has dire consequences, since  $m_s$  is always found to be over 600 MeV, while phenomenologically successful models typically have  $m_s \approx 500$  to 550 MeV. Figures 7 and 8 show the effects of varying the scalar mass from 500 MeV to 835 MeV with the nuclear matter properties held fixed (models E and F); we relax the preceding constraint on  $g_s$  to obtain the desired  $m_s$ . The vector mass

<sup>14</sup>We allow the second possibility to compensate for the tree-level value of  $g_A = 1$  within the model.

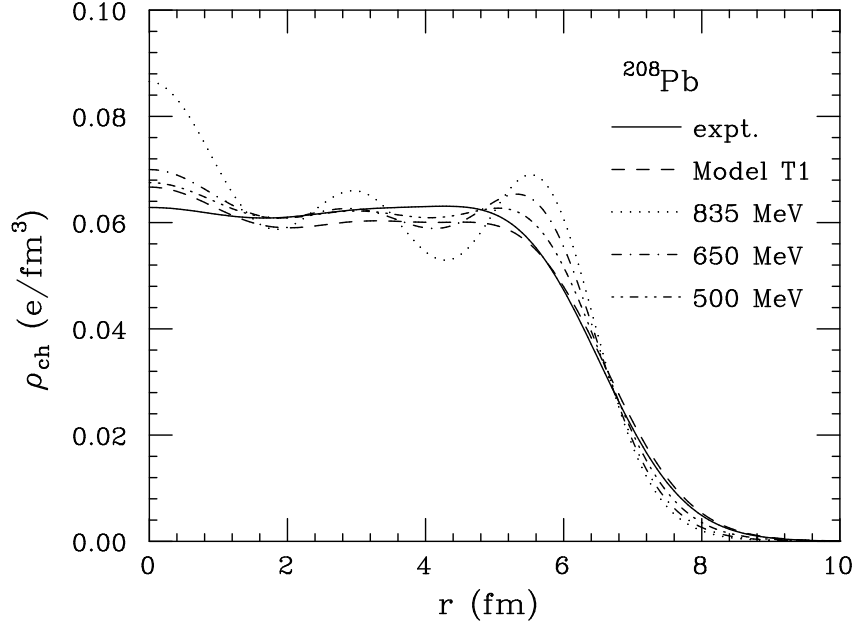


FIG. 7. Charge densities for chiral model E or F from Table III with three different scalar masses are compared to the density extracted from experiment. For comparison, model T1 from Ref. [36], which provides a good fit to properties of finite nuclei, is also shown.

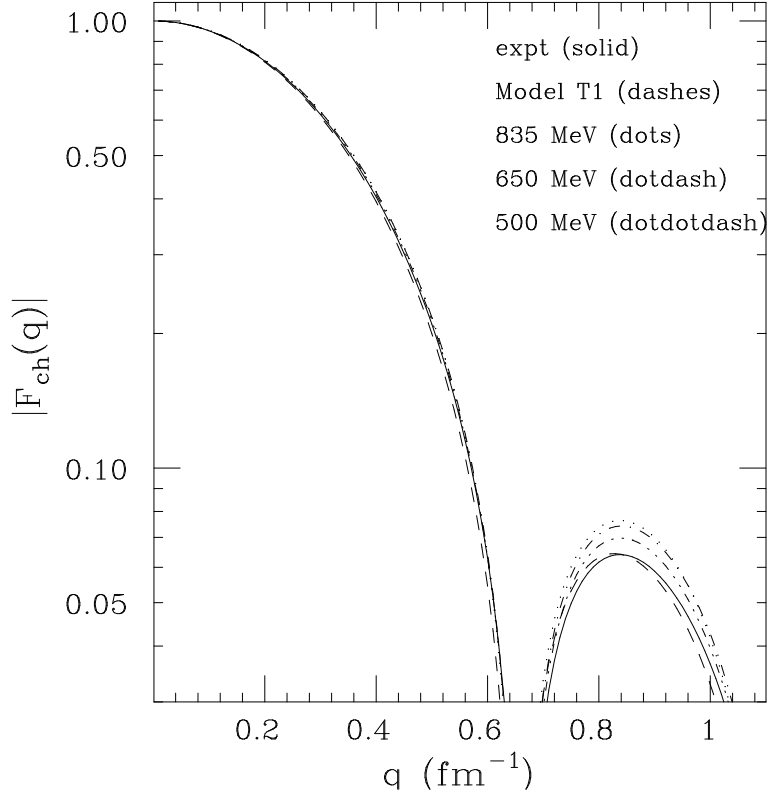


FIG. 8. Charge form factors  $|F_{\text{ch}}(q)|$  for chiral model E or F from Table III with three different scalar masses are compared to model T1 from Ref. [36] and experiment. The form factors are simply computed as the Fourier transforms of the charge densities in Fig. 7.



$m_v$  is also held fixed at its experimental value. Large scalar masses produce oscillations in the charge density (Fig. 7) or enhancements in the charge form factor (Fig. 8), which are not observed experimentally. Note that the experimental error bars in Fig. 8 are too small to include in the figure; the chiral curves are many standard deviations from the data at the second maximum. Moreover, the most unfavorable result shown ( $m_s = 835$  MeV) is the only one with an acceptable coupling, namely,  $g_s \approx g_\pi/g_A$ ; using the tree-level value  $g_s = g_\pi$  produces  $m_s = 1055$  MeV.

Other deficiencies are clearly revealed in calculations of finite nuclei, and this serves to validate our choice of desirable nuclear matter properties. Consider, for example, the single-particle spectrum near the Fermi surface in heavy nuclei. The large scalar masses required by the known value of  $g_s$  produce significant changes in the effective central potential seen by the nucleons. This is illustrated in Fig. 9. As the scalar mass increases, the slope of the potential in the nuclear surface becomes steeper; indeed, if one “averages out” the central oscillations, the dotted potential is essentially a square well. Thus, as the scalar mass increases, levels with large (nominal) values of the orbital angular momentum  $\ell$  become more deeply bound. This is illustrated in Fig. 10 by models E', E and F, which have scalar masses of 500 MeV, 650 MeV, and 835 MeV, respectively; the  $1h_{9/2}$  level, which should be unoccupied, is pushed down into the highest filled shell. Moreover, the large value of  $M_0^*/M \approx 0.8$  in these models reduces the spin-orbit splittings considerably, as can be seen by comparing the  $1h_{9/2}$ – $1h_{11/2}$  splitting in models E and F with the spectra in the successful models B and T1 (from Ref. [36]). The conclusion is that the large values of  $m_s$  and  $M_0^*/M$  obtained in the chiral models preclude a correct description of the shell closures in heavy nuclei.

If we are desperate to obtain a reasonable model of finite nuclei, we might abandon the connection to pion physics by decoupling  $g_s$  from  $g_\pi$ , so that  $m_s$  can be set near 500 MeV. This will produce reasonable charge densities and effective central potentials, as verified by Figs. 7 and 9. Nevertheless, the models are still restricted to the limited accessible region in Fig. 6, and the consequences are severe. The best that can be done is to reduce  $M_0^*/M$  as much as possible, so that the spin-orbit splittings are improved, and the single-particle level structure is reasonable. This is illustrated in Fig. 10 by model I (which exists at all densities) and model J (which disappears at  $\rho \approx 5\rho_0/4$ ); the lower values of  $m_s$  and  $M_0^*$  produce an acceptable level ordering and shell closure.

Unfortunately, the tradeoff in these models is also clear: the compression modulus  $K_0$  gets very large, and this disrupts the binding-energy systematics. This is illustrated in Fig. 11, where the deviation in the calculated surface energy ( $\delta a_2$ ) is plotted as a function of the compression modulus for different models. Here  $\delta a_2$  is determined by fitting the difference in the calculated<sup>15</sup> and experimental binding energies of  $^{16}\text{O}$ ,  $^{40}\text{Ca}$ , and  $^{208}\text{Pb}$  to a form  $\delta E = (\delta a_1)B + (\delta a_2)B^{2/3}$ . (We find  $\delta a_1 < 1$  MeV for all models. Other analyses give qualitatively similar results.) Apparently, models with compression moduli in the desirable range yield accurate surface energies, while the chiral models I and J clearly yield surface energies that are too large, roughly 40% larger than the observed value ( $a_2 \approx 18$  MeV).

Thus, by mapping out the accessible region in parameter space and by characterizing

---

<sup>15</sup>A center-of-mass correction is applied in determining the calculated binding energies [23].

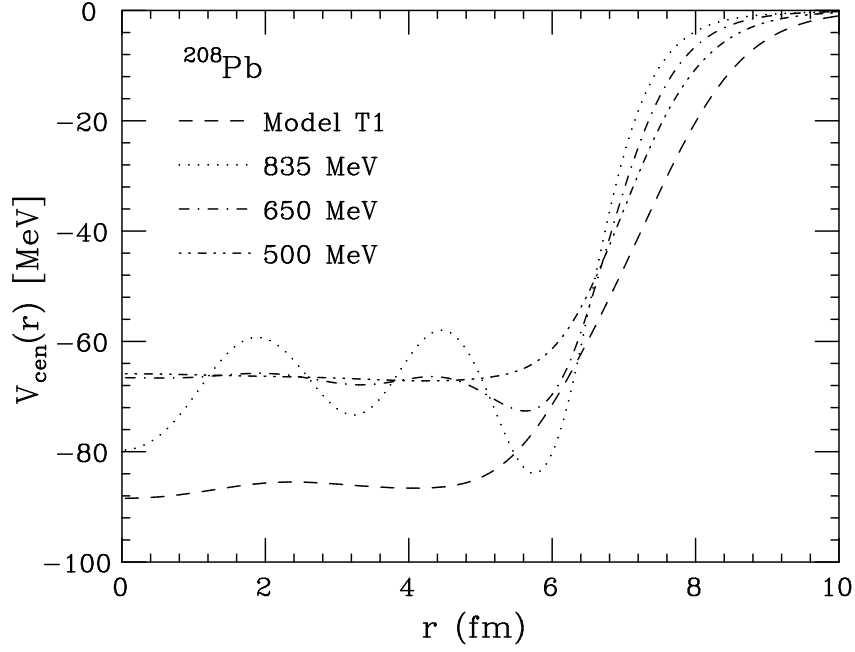


FIG. 9. Schrödinger-equivalent central potentials in  $^{208}\text{Pb}$  for model T1 from Ref. [36] and a chiral model (E,F) with three scalar masses  $m_s = 835$  MeV, 650 MeV, and 500 MeV.

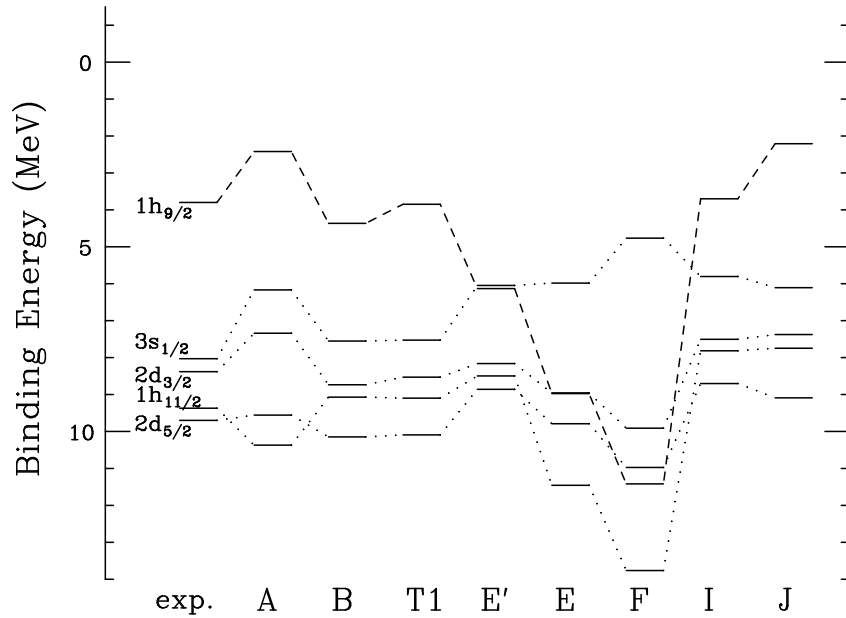


FIG. 10. Proton energy levels near the Fermi surface in  $^{208}\text{Pb}$ . Model T1 is from Ref. [36] and parameters for the others are given in Table III and in the text. (The scalar mass  $m_s = 500$  MeV in models I and J.)

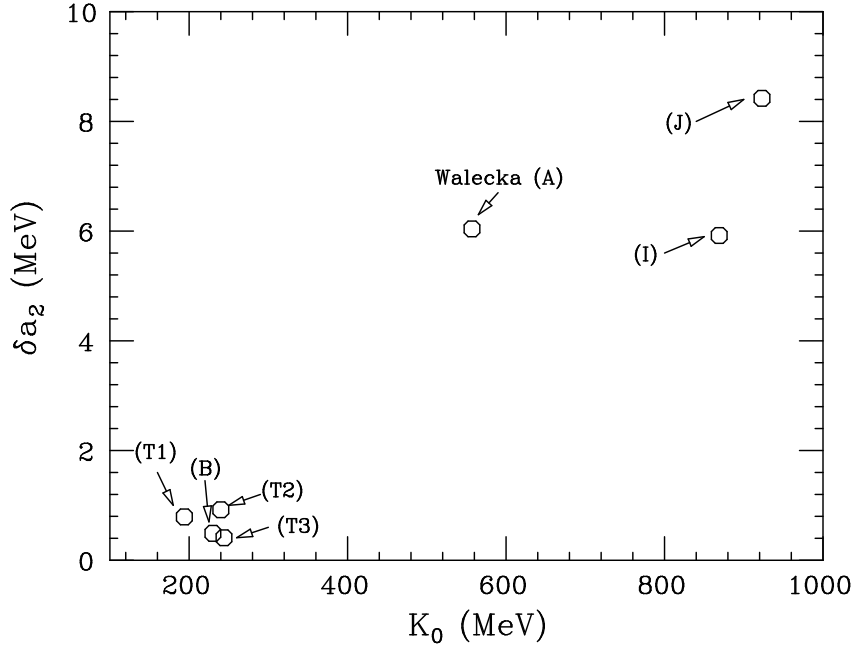


FIG. 11. Deviations in the surface energy  $\delta a_2$  (see text) *vs.* the compression modulus for the models T1, T2, and T3 from Ref. [36] and selected models from Table III.

the dependence of the nuclear observables on  $M_0^*$ ,  $K_0$ , and  $m_s$ , we conclude that models built upon the conventional linear sigma model and which feature a “Mexican-hat” potential cannot reproduce basic nuclear ground-state phenomenology at the Hartree level. The nuclear matter analysis of the simplest version (with  $\bar{\alpha} = \bar{\alpha}' = \zeta = 0$ ) shows that the constraints on the scalar self-couplings forced by the form of the scalar potential are incompatible with desirable equilibrium properties. Attempts to generate better properties by allowing  $\bar{\alpha} = \bar{\alpha}' > 0$  and  $\zeta > 0$  inevitably lead to Lee–Wick solutions with lower energy and to the absence of a normal solution at densities not far above equilibrium. The large value of  $g_s$  forced by the chiral constraint is an additional problem, since it requires the scalar mass to be too large.

A different realization of the chiral symmetry seems more compatible with observed nuclear properties and with successful relativistic mean-field models. Here one takes the chiral scalar mass to be *large* to eliminate the unphysical scalar nonlinearities and then generates the mid-range attractive force between nucleons *dynamically* through correlated two-pion exchange [62–66]. In principle, this approach can be realized within the models discussed above, albeit at the expense of much greater complexity, since one must first construct a boson-exchange kernel containing correlated two-pion exchange and then allow this kernel to act to all orders (for example, in a ladder approximation) to determine the NN interaction and the resulting nuclear matter energy density [39]. This calculation is further complicated by the necessity of maintaining chiral symmetry at finite density, which is difficult to do when one uses the non-derivative (“pseudoscalar”)  $\pi N$  coupling implied by the linear realization of the symmetry [8,67,68].

Alternatively, this approach can be implemented more easily with a *nonlinear* realization of the chiral symmetry. If desired, the mass of the heavy chiral scalar can be kept finite,

so that it plays the role of a regulator that maintains the renormalizability of the model [8], or the mass can be taken to infinity, so that the chiral scalar field decouples, resulting in the effective nonlinear model of Weinberg [32]. The strong scalar-isoscalar two-pion exchange can be simulated by adding a low-mass, “effective” scalar field coupled directly to the nucleon, and scalar self-interactions can be added to include a density dependence in the mid-range NN attractive force. The chiral symmetry is left intact, because the light scalar is an isoscalar, and the transformation rules on the nucleon field are nonlinear [68]. Since the pion mean field vanishes, the resulting chiral mean-field theory produces an energy functional just like the ones considered in Sec. II. Moreover, although the coupling strength  $g_s$  of the light scalar is comparable to  $g_\pi$  (as verified by explicit calculation of the correlated two-pion exchange [65,66]), we no longer require  $g_s = g_\pi$  and are free to adjust  $g_s$  within a reasonable range. In short, the general energy functionals studied earlier (including the Walecka model) are consistent with the underlying chiral dynamics of QCD, although its realization in nuclear physics is subtle. In the next section, we illustrate this scenario with a specific example from Ref. [36].

## V. CHIRAL MODELS THAT WORK

Here we discuss a chiral model that *can* successfully describe finite nuclei at the Hartree level. As we have seen, variants of the linear sigma model, with spontaneous symmetry breaking from a “Mexican-hat” potential, impose strong dynamical assumptions on the interactions of the light scalar.<sup>16</sup> In contrast, by working with a nonlinear representation of chiral symmetry, we remove these constraints, because the chiral-singlet scalar (which is called  $\sigma'$  by Weinberg [32]) can be decoupled from the other fields. We can then introduce a *new* chiral scalar to incorporate the dynamics in the scalar-isoscalar sector, as discussed at the end of the last section.

We consider the lagrangian from Ref. [36]:

$$\begin{aligned} \mathcal{L}(x) = & \bar{N} \left( i\gamma^\mu \mathcal{D}_\mu + g_A \gamma^\mu \gamma_5 a_\mu - M + g_s \phi + \dots \right) N - \frac{1}{4} (\partial_\mu V_\nu - \partial_\nu V_\mu)^2 \\ & + \frac{1}{2} \left[ 1 + \eta \frac{\phi}{S_0} + \dots \right] \left[ \frac{1}{2} f_\pi^2 \text{tr} (\partial_\mu U \partial^\mu U^\dagger) + m_v^2 V_\mu V^\mu \right] \\ & + \frac{1}{4!} \zeta (g_v^2 V_\mu V^\mu)^2 + \frac{1}{2} \partial_\mu \phi \partial^\mu \phi - H_q \left( \frac{S^2}{S_0^2} \right)^{2/d} \left( \frac{1}{2d} \ln \frac{S^2}{S_0^2} - \frac{1}{4} \right) + \dots, \end{aligned} \quad (81)$$

where  $g_A \approx 1.26$  is the axial coupling constant,  $\mathcal{D}_\mu = \partial_\mu + iv_\mu + ig_v V_\mu$  is a chirally covariant derivative, and  $U$ ,  $v_\mu$ , and  $a_\mu$  depend on the pion field (see Ref. [36] for details). Here we write the nucleon field as  $N$  to distinguish it from the field  $\psi$  used previously, because  $N$  transforms nonlinearly under the chiral symmetry. A novel feature of this model is that the scale dimension  $d$  of the new scalar field  $S(x)$  is allowed to differ from unity. The

---

<sup>16</sup>A linear sigma model variation, with spontaneous symmetry breaking from a logarithmic potential, *can* provide a good description of finite nuclei, as shown in Ref. [69].

scalar fluctuation field  $\phi$  is related to  $S$  by  $S(x) \equiv S_0 - \phi(x)$ . The form of the lagrangian is motivated by requiring that the model satisfy the low-energy theorems of broken scale invariance in QCD at the tree level in the effective scalar field. See Ref. [36] for more discussion of the motivation and consequences of Eq. (81).

This lagrangian illustrates one way to specify vacuum contributions, which at one-baryon-loop order modify all powers of  $\phi$ . The polynomial terms in  $\phi$  must be combined with corresponding counterterms; in this way, the vacuum contributions are absorbed into the renormalization of the scalar polynomial. In principle, there are an infinite number of unknown parameters. However, if one insists that the low-energy theorems are satisfied at tree level in the meson fields, the end result for the scalar potential must be of the form in Eq. (81), where the couplings are renormalized [36].<sup>17</sup> This potential can be expanded as a polynomial in  $\phi$  and *all* coefficients are determined by the three parameters  $S_0$ ,  $d$ , and  $H_q = m_s^2 d^2 S_0^2 / 4$ . One never has to explicitly calculate any counterterms; the nucleon-loop effects are automatically included in the scalar potential contained in Eq. (81). The assumption of naturalness provides an alternative (but not inconsistent) justification for limiting the impact of the quantum vacuum at ordinary density to the renormalization of a few parameters, as discussed below.

Thus we have only a few unknown renormalized constants (parameters); in Ref. [36] these were determined by fitting directly to finite nuclei, using a  $\chi^2$  minimization algorithm. Although we will not reproduce the results here, the charge densities, single-particle spectra, and binding-energy systematics are in good agreement with experiment. Moreover, the predicted nuclear matter equilibrium properties ( $e_0$ ,  $\rho_0$ ,  $M_0^*$ , and  $K_0$ ) fall within the desired ranges.

To connect this model with the present analysis, we present the energy density  $\mathcal{E}$  for uniform nuclear matter in the Hartree approximation:

$$\begin{aligned} \mathcal{E}(\phi, V_0; \rho_B) = & \frac{1}{4} m_s^2 S_0^2 d^2 \left\{ \left(1 - \frac{\phi}{S_0}\right)^{4/d} \left[ \frac{1}{d} \ln\left(1 - \frac{\phi}{S_0}\right) - \frac{1}{4} \right] + \frac{1}{4} \right\} + g_v \rho_B V_0 - \frac{1}{4!} \zeta(g_v V_0)^4 \\ & - \frac{1}{2} \left(1 + \eta \frac{\phi_0}{S_0}\right) m_v^2 V_0^2 + \mathcal{E}_k(\phi; \rho_B) , \end{aligned} \quad (82)$$

The parameter sets T1, T2, and T3 determined in Ref. [36] exhibit naturalness (see Sect. VI), as defined earlier; thus, if we expand the scalar potential in powers of  $\phi$ , terms beyond  $O(\phi^4)$  are unimportant (although not negligible) at nuclear densities and below, where  $\Phi/M \lesssim 0.4$ . With this truncation, the energy density becomes a special case of the general form considered earlier, and expressions for  $\bar{\kappa}$ ,  $\bar{\lambda}$ , and  $\bar{\alpha}$  are given in Table II.

This example illustrates that the general functional in Eq. (1) is consistent with the spontaneous breaking of chiral symmetry in QCD in a nonlinear realization. The key point is that chiral symmetry imposes no constraints on the scalar potential or the scalar-nucleon interaction, if a chiral-singlet scalar field generates the midrange attraction. (Of course,

---

<sup>17</sup>Another way to include vacuum effects is to insist on the renormalizability of the lagrangian. Then the first few powers of  $\phi$  are fixed by a set of renormalization conditions, and the higher powers contain finite, calculable coefficients.

all interaction terms must be isoscalars, and the nucleons must obey a nonlinear chiral transformation [32].) The lagrangian in Eq. (81) provides an explicit example of a model that is consistent with chiral symmetry (and broken scale invariance) and that produces accurate results for finite nuclei in the Hartree approximation; moreover, the coefficients are natural, thus allowing for a truncation of the energy functional. In contrast to linear chiral models with “Mexican-hat” potentials, the logarithmic potential in Eq. (82) allows for relatively weak scalar nonlinearities and the dominance of the cubic and quartic terms with reasonable values of the scaling dimension  $d$ ; the coefficients of the scalar terms are natural as a result. Although the logarithmic form was motivated by considering the broken scale invariance of QCD, we could equally well impose as a *phenomenological principle* that the coefficients in the energy functional be natural, since the subsequent truncation leads to similar results. In short, the energy functionals considered in Sec. II are consistent with spontaneously broken chiral symmetry, the broken scale invariance of QCD, and the basic observed properties of finite nuclei.

## VI. DISCUSSION

Descriptions of nuclear matter and finite nuclei, which are ultimately governed by the physics of low-energy QCD, are efficiently formulated using low-energy degrees of freedom, namely, the hadrons. The application of effective field theory methods to nuclear physics problems, however, is in its adolescence, with new developments occurring rapidly. In this work, we try to build upon the success of relativistic mean-field phenomenology by using ideas from density functional theory and effective field theory. One of the key issues is *naturalness*.

As noted earlier, we have excluded many terms from our energy functional: higher-order polynomials in the vector fields and mixed scalar–vector terms, derivative terms, and so on. In retrospect, were we justified in neglecting them? An important assumption in applying effective field theories, such as chiral perturbation theory, is that the coefficients of terms in the lagrangian are “natural”, *i.e.*, of order unity, when written in appropriate dimensionless units. This assumption permits the organization of terms through a power-counting scheme, because one can systematically truncate the expansion when working to a desired level of accuracy [33]. We propose an analogous concept of naturalness for the energy functional, which will justify the neglect of higher derivatives and powers of the fields when applying Eq. (1) to nuclei. This is the basic idea that underlies our effective field theory approach to the nuclear many-body problem.

In performing a mean-field analysis [18,40], one can easily identify dimensionless ratios that set the scale of individual contributions to the energy. For example, one can rewrite the scaled energy density of nuclear matter,  $\mathcal{E}/M^4$ , in terms of the dimensionless ratios  $g_v V_0/M = W/M$  and  $g_s \phi/M = \Phi/M$ , which then become our finite-density expansion parameters. If one expresses the nuclear matter energy density in terms of the scaled field variables written above [see Eqs. (20)–(22)], one finds that the ratios

$$\frac{1}{2c_v^2 M^2}, \quad \frac{1}{2c_s^2 M^2}, \quad \frac{\bar{\kappa}}{6M}, \quad \frac{\bar{\lambda}}{24}, \quad \frac{\zeta}{24}, \quad \bar{\alpha}, \quad \dots \quad (83)$$

TABLE IV. Dimensionless ratios of Eq. (83) evaluated in the models of Ref. [36]. The absolute values are shown, and all have been multiplied by  $10^3$ .

Model	$\frac{1}{2c_s^2 M^2}$	$\frac{1}{2c_v^2 M^2}$	$\frac{\bar{\kappa}}{6M}$	$\frac{\bar{\lambda}}{24}$	$\frac{\zeta}{24}$	$\bar{\alpha}$
T1	1.48	2.25	0.02	0.03	1.68	1.16
T2	1.65	2.52	0.35	0.12	1.43	1.77
T3	1.34	1.95	0.32	0.13	1.44	0.31

should all be of roughly equal size (or at least of the same order of magnitude) for our expansion to be “natural”.

In Table IV, we illustrate these ideas using parameter sets T1, T2, and T3 from Ref. [36]. These sets accurately reproduce nuclear properties, and we observe that the parameters are consistent with our definition of naturalness. The nonlinear scalar parameters tend to be somewhat small, but it is clear that one can shift strength between terms with equal powers of the meson fields, which follows because both  $\Phi$  and  $W$  are roughly proportional to  $\rho_B$ . Thus, to make concrete conclusions about the importance of nonlinearities, one should include all terms consistent with the level of truncation. (Note, however, that the quartic parameter  $\bar{\alpha}'$  was set to zero in Ref. [36]; when it is included in a fit, the optimal parameter set becomes *more* natural.) Observe also the important result that the highest-order terms retained ( $\zeta$ ,  $\bar{\lambda}$ ) do not dominate the energy.

The usefulness of naturalness extends to gradient terms, which do not contribute in uniform nuclear matter. Experience with mean-field models applied to finite nuclei shows that the derivatives of the fields are small; one finds that typically,  $|\nabla\Phi|/M^2$  and  $|\nabla W|/M^2$  are  $(0.2)^2$  or less. If we assume mean-field dominance, such that fluctuations around the mean fields are small, and the naturalness of the coefficients in the derivative expansion, we can truncate the derivative terms at some tractable order. In the models studied here we consider only quadratic terms in gradients of the fields.

Naturalness implies that we should not expect qualitative changes in our description from additional higher-order terms. If the physics is consistently dictated by the last terms added, the system (or framework) is not natural. Further support for the naturalness assumption in our framework comes from extending the model in Ref. [36] to include  $\phi^2 V_\mu V^\mu$  and  $(V_\mu V^\mu)^3$  terms and then repeating an optimization directly to selected properties of finite nuclei. The new fits are very close to the fits obtained without these terms. Furthermore, contributions to the energy from the new terms are less than 10% of those from the old terms at nuclear matter density, and the old coefficients change only slightly in the new fit [40]. Thus contributions from the higher-order terms can be absorbed into slight adjustments of the coefficients in Eq. (81). Moreover, since the terms quadratic in gradients of the field are small, one expects that adding additional field gradients will produce only minor effects.

Naturalness also implies that we can exploit the freedom to make nonlinear field redefinitions. Although we have no general proof that finite-density observables are unchanged under these redefinitions, it is certainly true at the mean-field level (*i.e.*, with classical meson fields). This freedom allows us to show that our couplings to the nucleon field are more general than is apparent at first. For example, if instead of  $g_s \bar{\psi} \phi \psi$  we have  $g_s \bar{\psi} f(\phi) \psi$ , with

$f(\phi) = \phi + \dots$ , we can redefine the scalar field to recover our standard form. Similarly, we can reproduce contact interactions among the nucleons by appropriately choosing nonlinear interactions among the meson fields; eliminating the meson fields using the field equations then provides the desired products of nucleon densities and currents. Thus there are numerous ways to write the energy functional that produce equivalent results, provided one keeps all orders in the interaction terms. The basic question is which representation leads to the most efficient truncation scheme, namely, one with meaningful dimensionless expansion parameters, that can be truncated at low order and still provide an accurate description of empirical data, using “natural” coefficients. Whereas we cannot say that other ways of writing the energy functional will not be useful [70], we have at least found one way of parametrizing the interactions (simple Yukawa meson–nucleon couplings with additional nonlinear couplings between meson fields) that satisfies the desired constraints. These issues will be discussed further in Ref. [40].

One might instead decide to parametrize the nuclear matter energy density by simply expanding in powers of the Fermi momentum  $k_F$  and by adjusting the coefficients in this expansion to the desired nuclear matter properties. In practice, this is neither efficient nor illuminating. One finds that to reproduce accurately the density dependence found in successful models, one must include many terms in the expansion [roughly through  $O(k_F^{14})$  in  $\mathcal{E}/\rho_B$ ]. Moreover, even with this many terms, extrapolations to higher density are problematic. If all of the coefficients were independent, they would not be sufficiently constrained by the few conditions on nuclear matter near equilibrium. In contrast, in models with meson fields, the parameters are correlated, and these constraints are effective in restricting the relevant region of parameter space.

If one accepts the validity of our assumption of naturalness, we can compare our truncated energy functional to one obtained directly from the Hartree (or one-baryon-loop) approximation to a given lagrangian. Although both approaches lead to Dirac equations for nucleons moving in local meson fields, the parameters in the energy functional and in the lagrangian may actually be related in a complicated fashion. The basic premise of density functional theory is that it is possible to parametrize exchange and two-nucleon correlation effects through local (Kohn–Sham) potentials (or self-energies), and that is how we may interpret our local meson fields.

This approach is useful, however, only for ground-state properties like the total energy and particle densities, and in general, the single-particle wave functions and eigenvalues are simply mathematical constructs that have no direct relation to observables. Fortunately, relativistic calculations including exchange and two-nucleon correlations show that the Hartree contributions dominate the self-energies, which are essentially state independent. Thus we expect that the large scalar and vector fields seen at the Hartree level will control the dynamics, and that the majority of exchange and correlation effects can be included by adjusting the nonlinear parameters (and thereby the density dependence) contained in the energy functional; this “Hartree dominance” also makes it reasonable to compare the single-particle energies with observed spectra, at least for states near the Fermi surface. These considerations again indicate the efficiency of writing the energy functional in terms of self-interacting meson fields: at normal nuclear densities these fields are small enough compared to the nucleon mass to provide useful expansion parameters, yet large enough that exchange and correlation corrections can be included, at least approximately, as minor perturbations.



Although this mean-field approach allows for an accurate description of many nuclear properties and has been applied to various regions of the Periodic Table, it is really just the first step in the development of a systematic treatment of the relativistic nuclear many-body problem based on effective field theory. There are many limitations and unsolved problems. First, there is the question of a more complete inclusion of higher-order corrections in the energy functional. These could be computed by starting with a lagrangian whose parameters are fit to NN data and then by calculating at a similar level (for example, DBHF) at finite density. Although it is known that one can parametrize the density dependence of the DBHF self-energies with meson self-interactions [42], and that one can include rearrangement effects consistently in the single-particle Dirac equations [54], the state dependence of the self-energies is neglected in these calculations. By comparing results of more sophisticated nuclear matter calculations with their mean-field parametrizations, one may be able to optimize the description of state-dependent effects, which will be important if one wants to study the nucleon–nucleus optical potential at high energy, for example.

The description of the quantum vacuum should also be improved. As discussed earlier, it is possible to include these effects at the one-loop level by incorporating them into the model parameters; if our naturalness assumption is valid, only a few such parameters are needed in practice. Higher-order contributions, however, will require counterterms involving fermion fields and will introduce vacuum contributions that explicitly involve the valence nucleons (the strong Lamb shift, for example). Moreover, the present approach neglects contributions from meson loops.

One must also consider the limitations of the present model, particularly with regard to extrapolation to high density. At nuclear densities and below, we have seen that only a few terms are needed in the energy functional to describe nuclei, and that the sensitivity to higher-order products of fields is minimal. This precludes a determination of the coefficients of these higher-order terms from empirical data. As the density increases, however,  $\Phi/M$  and  $W/M$  increase accordingly, and the unknown higher-order terms may become important. This prevents a controlled extrapolation to high densities, such as those relevant in the interiors of neutron stars. It is not clear at present what the limits to reliable extrapolation are. These difficulties are shared by all existing treatments of the nuclear many-body problem in terms of hadrons; for example, calculations of few-nucleon systems based on nonrelativistic potentials [71,72] are sensitive to three-body (and perhaps four-body) forces, but reliable extrapolation to high density is likely to require information on additional many-body forces as well.

To close the discussion, we return to the question of whether the nuclear properties considered here lead to additional constraints on the nuclear matter saturation curve near equilibrium. As noted in Sec. II, some recent work indicates that the ratio of the “skewness”  $S$  to the compression modulus  $K$  is constrained by monopole vibrations [59,60]. To study this issue, we considered an energy functional of the form in Eq. (1) with  $\alpha = \alpha' = 0$  and varied the ratio  $(S/K)_0$  by varying  $\zeta$  while holding all other nuclear matter inputs fixed. We found little correlation between the value of  $(S/K)_0$  and the nuclear observables studied here; for example, in Fig. 12, we show the proton levels near the Fermi surface in  $^{208}\text{Pb}$  from five models for which  $(S/K)_0$  ranges by more than a factor of five. As long as the parameter set is natural, the effects of varying the skewness are small, and similar results were found for other observables. These results support Bodmer’s conjecture [18] that the

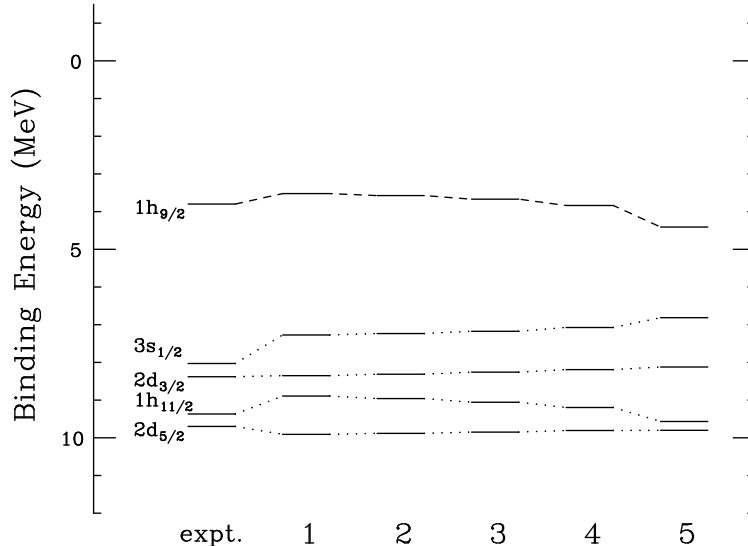


FIG. 12. Single-particle proton levels near the Fermi surface in  $^{208}\text{Pb}$  for five models with fixed  $e_0$ ,  $\rho_0$ ,  $M_0^*$ , and  $K_0$ , but different  $(S/K)_0$ .

spin-orbit splittings in nuclei are determined essentially by  $M_0^*$  and are independent of the specific form of the nonlinear interactions.

## VII. SUMMARY

In this paper, we demonstrate that it is impossible to unite relativistic mean-field phenomenology with manifest chiral symmetry by building upon the conventional linear sigma model, which contains a “Mexican-hat” potential and a light scalar meson playing a dual role as the chiral partner of the pion *and* the mediator of the intermediate-range NN attraction. We illustrate the generic failure of this type of model at the Hartree level as well as the characteristics of chiral models that *can* successfully describe finite nuclei.

Although our study of chiral models involves specific lagrangians treated at the Hartree (or one-baryon-loop) level, the analysis is based on the more general concept of an energy functional that describes the finite, many-nucleon system. The energy functional depends on valence-nucleon Dirac wave functions and classical scalar and vector meson fields. We interpret this energy functional within the framework of density functional theory, which says that the exact energy functional for the system can be written entirely in terms of the scalar density and baryon four-current density. Rather than work solely in terms of densities, we include auxiliary meson fields, which correspond to (local) Kohn–Sham potentials, and which provide an efficient parametrization of the density dependence. Thus, with a sufficiently general energy functional, we can include many-body effects beyond the simple Hartree level, even though we retain only classical meson fields and local interactions. Rather than attempt to compute the form of the functional directly from an underlying lagrangian, we use observed nuclear properties (and extrapolations to nuclear matter) to determine the unknown coefficients.

In the general case, the energy functional contains an infinite number of interaction terms

involving the nucleon and meson fields, and their derivatives. This is actually an advantage, since transformations of the field variables allow one to cast the functional in different forms, with the goal being to find the representation that allows the most efficient truncation. For the truncation to be plausible, one must have a reasonable (small) expansion parameter, and one must assume a principle of “naturalness”, which says that the coefficients of the expansion, when written in appropriate dimensionless ratios, must all be of order unity. These are precisely the basic ideas underlying applications of effective field theories, such as chiral perturbation theory. We showed that such a truncation of the energy functional is possible at and below normal nuclear densities, if the functional is written in terms of self-interacting scalar and vector fields with Yukawa couplings to the nucleons; under these conditions, the ratios of the meson fields (and their gradients) to the nucleon mass are small enough to serve as useful expansion parameters, and sets of coefficients can be found that both reproduce observed nuclear properties and satisfy the naturalness assumption. In practice, truncation of the energy functional at quartic terms in the meson fields and at quadratic terms in field gradients is sufficient for the observables studied here.

To constrain the energy functional, we use nuclear observables that are meaningful from the standpoint of the underlying density functional framework, such as (charge) densities and total binding energies. Although in general, the single-particle Dirac eigenvalues obtained in the local potentials are not directly related to observables, we note that in the relativistic nuclear many-body problem, the single-particle potentials (or self-energies) are known to be dominated by the Hartree contributions and are essentially state independent. Thus the exchange and correlation effects included in the potentials are small, and it is reasonable to also use observed nuclear spectra as input, at least for states near the Fermi surface. In short, the observables we use to constrain the parameters are precisely the ones that should be calculable in a density functional framework where the Hartree terms dominate the self-energies. We also observe the fortunate result that the scalar and vector fields are small enough compared to the nucleon mass to serve as useful expansion parameters, yet large enough that exchange and correlation effects enter only as small perturbations (at least for occupied states).

Rather than fit directly to the properties of finite nuclei, we extrapolate instead and determine our parameters from the properties of nuclear matter near equilibrium. In nuclear matter, the energy functional reduces to a function of the Fermi momentum and the (constant) scalar and vector fields; it is then possible to invert the field equations and express the unknown parameters directly in terms of the nuclear matter “observables”. This allows us to scan the parameter space to find sets that lead to an accurate reproduction of nuclear properties. More importantly, we can exclude models that are too constrained (by symmetry, for example) by showing that it is impossible for them to reproduce desirable nuclear matter results.

Parameter sets that accurately reproduce nuclear observables typically involve small but significant nonlinear meson self-interactions. These self-interactions introduce additional density dependence beyond that contained in simple Yukawa meson–nucleon couplings. This density dependence can be interpreted either in terms of meson masses that are modified in the nuclear medium or in terms of variations in the scalar and vector self-energies. We can make three important observations about this additional density dependence: First, it can be parametrized efficiently using self-interactions of the meson fields. Second, to make

meaningful statements about the size of these self-interactions, one must include all allowed terms at the given level of truncation, as required by naturalness. This is relevant since most relativistic mean-field calculations to date have concentrated on scalar self-interactions only, omitting scalar–vector and vector–vector terms. Third, although we choose to determine these interactions by fitting to empirical nuclear properties, one could instead fit them to the results of more detailed nuclear matter calculations based on an underlying lagrangian, such as DBHF. If the DBHF self-energies are determined from fits to NN observables, this alternative procedure provides a direct link between relativistic finite-nucleus structure calculations and the two-nucleon problem.

To address the chiral models, we considered specific lagrangians that realize the spontaneously broken chiral symmetry of QCD in different ways and studied them at the Hartree level. The resulting energy functionals are special cases of the general one studied earlier, so we apply our previous analysis and test whether acceptable parametrizations can be obtained. We find that the accessible region for linear sigma models is far from the region of acceptable nuclear phenomenology. The results of this new analysis solidify our previous conclusion [17] that chiral hadronic models built upon the conventional linear sigma model cannot reproduce observed properties of finite nuclei, at least at the Hartree level. The two critical constraints imposed by the conventional lagrangian are the “Mexican-hat” potential and the connection between the scalar coupling and the pion coupling ( $g_s = g_\pi/g_A$ ). The former generates scalar self-interactions with the wrong systematics, and the latter produces a scalar mass that is too large, leading to unrealistic nuclear charge densities, level orderings, and shell closures.

On the other hand, one can find chiral models that *are* phenomenologically successful at the Hartree level. As an example, we discuss a model that was introduced in a recent paper, which features a nonlinear realization of chiral symmetry. One motivation for such a model is that the chiral scalar present in the linear sigma model is irrelevant for the nuclear dynamics; the mid-range NN attraction arises instead from the exchange of two correlated pions. One can simulate this attraction by introducing an auxiliary scalar field with a Yukawa coupling to the nucleon. Chiral symmetry is maintained if the nucleon field transforms nonlinearly and the auxiliary field is a chiral scalar. Due to the nonlinear realization of the symmetry, the “Mexican-hat” potential is no longer needed, and various constraints on the model parameters disappear. At the Hartree level, the energy functional has the full flexibility of the general functional considered earlier; thus, parameter sets can be found that accurately reproduce nuclear properties in a framework that is consistent with the underlying chiral symmetry of QCD. Moreover, we observe that successful models have parameters that are consistent with our “naturalness” assumption, which forms the basis for our expansion and truncation scheme.

Although the general mean-field approach studied here leads to excellent results for the bulk properties of nuclei, there are many questions to be answered before one has a consistent, systematic treatment of the relativistic nuclear many-body problem. A more accurate inclusion of vacuum, exchange, and correlation effects should be pursued. The extension of this framework to deal with high-density matter, where the expansion parameters are no longer small, is also an outstanding problem. Some of these ideas will be discussed in a future paper [40].

## ACKNOWLEDGMENTS

We thank P. Ellis, H. Müller, and J. Rusnak for useful comments and stimulating discussions. We also acknowledge the Institute for Nuclear Theory at the University of Washington, where part of this work was carried out. This work was supported in part by the Department of Energy under Contract No. DE-FG02-87ER40365, the National Science Foundation under Grants No. PHY-9203145 and PHY-9258270, and the A. P. Sloan Foundation.

## REFERENCES

- [1] J. Schwinger, *Ann. Phys. (N.Y.)* **2** (1957) 407
- [2] M. Gell-Mann and M. Lévy, *Nuovo Cim.* **16** (1960) 705
- [3] B. W. Lee, *Chiral Dynamics* (Gordon and Breach, New York, 1972)
- [4] T. D. Lee and G. C. Wick, *Phys. Rev. D* **9** (1974) 2291
- [5] A. K. Kerman and L. D. Miller, Second High-Energy Heavy Ion Summer Study, Lawrence Berkeley Laboratory report LBL-3675 (1974) (unpublished)
- [6] E. M. Nyman and M. Rho, *Phys. Lett.* **60B** (1976) 134
- [7] E. M. Nyman and M. Rho, *Nucl. Phys.* **A268** (1976) 408
- [8] T. Matsui and B. D. Serot, *Ann. Phys. (N.Y.)* **144** (1982) 107
- [9] J. Boguta, *Phys. Lett.* **120B** (1983) 34; **128B** (1983) 19
- [10] A. D. Jackson, M. Rho, and E. Krotscheck, *Nucl. Phys.* **A407** (1983) 495
- [11] S. Sarkar and S. K. Chowdhury, *Phys. Lett.* **153B** (1985) 358
- [12] J. Kunz, D. Masak, U. Post, and J. Boguta, *Phys. Lett.* **169B** (1986) 133
- [13] J. Kunz, D. Masak, and U. Post, *Phys. Lett.* **186B** (1987) 124
- [14] J. Boguta, *Nucl. Phys.* **A501** (1989) 637
- [15] V. N. Fomenko, S. Marcos, and L. N. Savushkin, *J. Phys. G* **19** (1993) 545
- [16] V. N. Fomenko, L. N. Savushkin, S. Marcos, R. Niembro, and M. L. Quelle, *J. Phys. G* **21** (1995) 53
- [17] R. J. Furnstahl and B. D. Serot, *Phys. Rev. C* **47** (1993) 2338; *Phys. Lett. B* **316** (1993) 12
- [18] A. R. Bodmer, *Nucl. Phys.* **A526** (1991) 703
- [19] C. J. Horowitz and B. D. Serot, *Nucl. Phys.* **A368** (1981) 503
- [20] B. D. Serot and J. D. Walecka, *Adv. Nucl. Phys.* **16** (1986) 1
- [21] P.-G. Reinhard, M. Rufa, J. Maruhn, W. Greiner, and J. Friedrich, *Z. Phys.* **A323** (1986) 13
- [22] R. J. Furnstahl, C. E. Price, and G. E. Walker, *Phys. Rev. C* **36** (1987) 2590
- [23] P.-G. Reinhard, *Rep. Prog. Phys.* **52** (1989) 439
- [24] Y. K. Gambhir, P. Ring, and A. Thimet, *Ann. Phys. (N.Y.)* **198** (1990) 132
- [25] B. D. Serot, *Rep. Prog. Phys.* **55** (1992) 1855
- [26] M. M. Sharma, M. A. Nagarajan, and P. Ring, *Phys. Lett. B* **312** (1993) 377
- [27] M. M. Sharma, G. A. Lalazissis, and P. Ring, *Phys. Lett. B* **317** (1993) 9
- [28] R. M. Dreizler and E. K. U. Gross, *Density Functional Theory* (Springer, Berlin, 1990)
- [29] C. Speicher, R. M. Dreizler, and E. Engel, *Ann. Phys. (N.Y.)* **213** (1992) 312
- [30] R. N. Schmid, E. Engel, and R. M. Dreizler, *Phys. Rev. C* **52** (1995) 164
- [31] E. Engel, H. Müller, C. Speicher, and R. M. Dreizler, *in* NATO Advanced Science Institute Series B, vol. 337, eds. E. K. U. Gross and R. M. Dreizler (Plenum, New York, 1995)
- [32] S. Weinberg, *Phys. Rev. Lett.* **18** (1967) 188
- [33] H. Georgi, *Annu. Rev. Nucl. Part. Sci.* **43** (1993) 209
- [34] S. Weinberg, *The Quantum Theory of Fields*, vol. I: Foundations (Cambridge Univ. Press, New York, 1995)
- [35] W. Kohn and L. J. Sham, *Phys. Rev. A* **140** (1965) 1133
- [36] R. J. Furnstahl, H. B. Tang, and B. D. Serot, *Phys. Rev. C* **52** (1995) 1368

- [37] C. J. Horowitz and B. D. Serot, Nucl. Phys. **A464** (1987) 613; **A473** (1987) 760 (E)
- [38] B. ter Haar and R. Malfliet, Phys. Rep. **149** (1987) 207
- [39] R. Machleidt, Adv. Nucl. Phys. **19** (1989) 189
- [40] R. J. Furnstahl, B. D. Serot, and H. B. Tang, in preparation
- [41] J. Boguta and A. R. Bodmer, Nucl. Phys. **A292** 413 (1977)
- [42] S. Gmuca, Z. Phys. A **342** (1992) 387; Nucl. Phys. **A547** (1992) 447
- [43] H. Kouno, K. Koide, T. Mitsuimori, N. Noda, A. Hasegawa, and M. Nakano, Phys. Rev. C **52** (1995) 135
- [44] J. D. Walecka, Ann. Phys. (N.Y.) **83** (1974) 491
- [45] S. A. Chin, Ann. Phys. (N.Y.) **108** (1977) 301
- [46] C. J. Horowitz and B. D. Serot, Phys. Lett. **137B** (1984) 287
- [47] L. I. Schiff, Phys. Rev. **84** (1951) 1, 10
- [48] A. R. Bodmer and C. E. Price, Nucl. Phys. **A505** (1989) 123
- [49] G. Velo and D. Zwanzinger, Phys. Rev. **188** (1969) 2218
- [50] G. Velo, Nucl. Phys. **B65** (1973) 427
- [51] V. I. Ogievetskij and I. V. Polubarinov, Ann. Phys. (NY) **25** (1963) 358
- [52] J. Zimanyi and S. A. Moskowski, Phys. Rev. C **42** (1990) 1416
- [53] A. Delfino, C. T. Coelho, and M. Malheiro, Phys. Rev. C **51** (1994) 2188
- [54] H. Lenske and C. Fuchs, Phys. Lett. B **345** (1995) 355
- [55] A. Bohr and B. R. Mottelson, Nuclear Structure, Vol. I (Benjamin, New York, 1969)
- [56] A. L. Fetter and J. D. Walecka, Quantum Theory of Many-Particle Systems (McGraw-Hill, New York, 1971)
- [57] C. F. von Weizsäcker, Z. Phys. **96** (1935) 431
- [58] P. A. Seeger and W. M. Howard, Nucl. Phys. **A238** (1975) 491
- [59] J. M. Pearson, Phys. Lett. B **271** (1991) 12
- [60] S. Rudaz, P. J. Ellis, E. K. Heide, and M. Prakash, Phys. Lett. B **285** (1992) 183
- [61] G. A. Lalazissis and M. M. Sharma, Nucl. Phys. **A586** (1995) 201
- [62] A. D. Jackson, D. O. Riska, and B. Verwest, Nucl. Phys. **A249** (1975) 397
- [63] J. W. Durso, M. Saarela, G. E. Brown, and A. D. Jackson, Nucl. Phys. **A278** (1977) 445
- [64] J. W. Durso, A. D. Jackson, and B. J. VerWest, Nucl. Phys. **A345** (1980) 471
- [65] W. Lin and B. D. Serot, Phys. Lett. **233B** (1989) 23
- [66] W. Lin and B. D. Serot, Nucl. Phys. **A512** (1990) 637
- [67] C. J. Horowitz and B. D. Serot, Phys. Lett. **108B** (1982) 377
- [68] J. D. Walecka, Theoretical Nuclear and Subnuclear Physics (Oxford Univ. Press, New York, 1995) chs. 22 and 23
- [69] E. K. Heide, S. Rudaz, and P. J. Ellis, Nucl. Phys. **A571** (1994) 713
- [70] T. H. R. Skyrme, Phil. Mag. **1** (1956) 1043; T. H. R. Skyrme, Nucl. Phys. **9** (1959) 615; M. Beiner, H. Flocard, N. Van Giai, and P. Quentin, Nucl. Phys. **A238** (1975) 29
- [71] R. B. Wiringa, Phys. Rev. C **43** (1991) 1585
- [72] J. Carlson, *in* Structure of Hadrons and Hadronic Matter, eds. O. Scholten and J. H. Koch (World Scientific, Singapore, 1991), p. 43